doi:10.1038/nature12080

Supplementary Figures

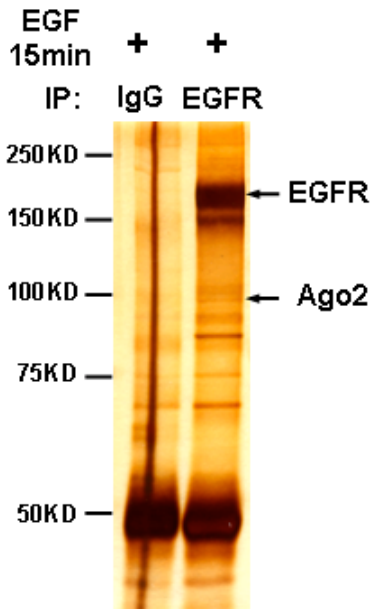

Supplementary Figure 1. Ago2 is a novel EGFR-interacting protein, in addition to those previously reported[28]. Immunoprecipitation was performed in serum-starved EGF treated HeLa cells (with moderate expression of EGFR) with IgG control or anti-EGFR antibody Ab-13. Unique peptides of Argonarute2 were identified by mass spectrometric analysis in EGFR-immunoprecipitated protein sample, as shown by silver staining of the representative purification of endogenous EGFR.

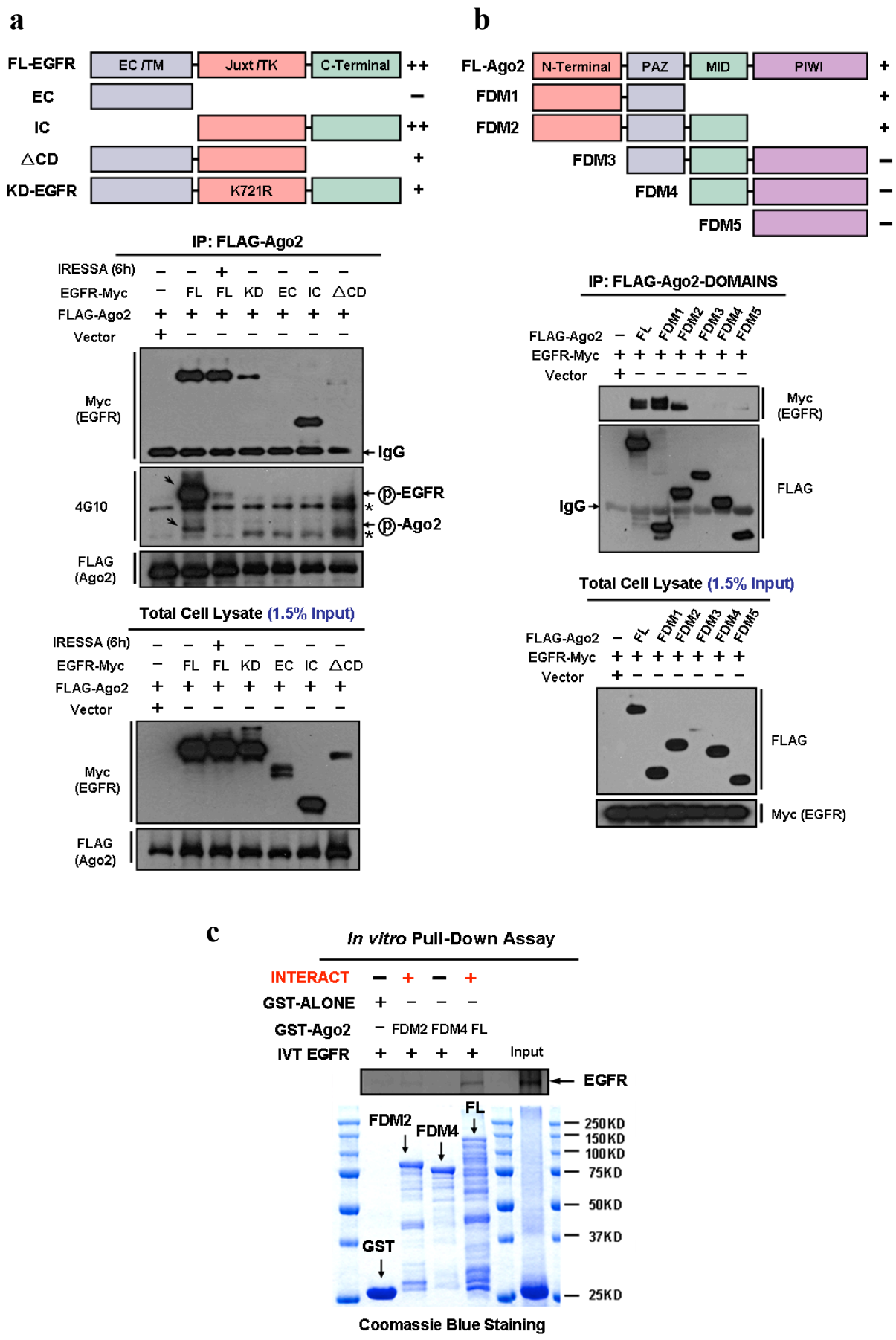
a
FL-EGFR
EC /TM
Juxt /TK
C-Terminal
++
EC
−
IC
++
△CD
+
KD-EGFR
K721R
+
IP: FLAG-Ago2
IRESSA (6h) − − + − − − −
EGFR-Myc − FL FL KD EC IC △CD
FLAG-Ago2 + + + + + + +
Vector + − − − − − −
Myc (EGFR)
IgG
4G10
ⓟ-EGFR
ⓟ-Ago2
FLAG (Ago2)
Total Cell Lysate (1.5% Input)
IRESSA (6h) − − + − − − −
EGFR-Myc − FL FL KD EC IC △CD
FLAG-Ago2 + + + + + + +
Vector + − − − − − −
Myc (EGFR)
FLAG (Ago2)
b
FL-Ago2
N-Terminal
PAZ
MID
PIWI
+
FDM1
+
FDM2
+
FDM3
−
FDM4
−
FDM5
−
IP: FLAG-Ago2-DOMAINS
FLAG-Ago2 − FL FDM1 FDM2 FDM3 FDM4 FDM5
EGFR-Myc + + + + + + +
Vector + − − − − − −
Myc (EGFR)
IgG
FLAG
Total Cell Lysate (1.5% Input)
FLAG-Ago2 − FL FDM1 FDM2 FDM3 FDM4 FDM5
EGFR-Myc + + + + + + +
Vector + − − − − − −
FLAG
Myc (EGFR)
c
In vitro Pull-Down Assay
INTERACT − + − +
GST-ALONE + − − −
GST-Ago2 − FDM2 FDM4 FL
IVT EGFR + + + + Input
EGFR
FDM2
FDM4
FL
GST
250KD
150KD
100KD
75KD
50KD
37KD
25KD
Coomassie Blue Staining

Supplementary Figure 2. EGFR Juxt/Kinase domain and the N-terminal region of Ago2 are required for direct protein-protein association. a, FLAG-tagged Ago2 was co-expressed with vector-control, full-length EGFR (with or without Iressa treatment), Kinase-Dead $EGFR^{K721R}$ or different functional domains in 293T cells. Anti-FLAG immunoprecipitates were blotted with myc antibody to show the interaction between EGFR and Ago2. The efficacy of Iressa (tyrosine kinase inhibitor targeting EGFR) treatment was verified by the reduced tyrosine phosphorylation of EGFR. * indicates the non-specific signal recognized by FLAG antibody. **b,** Myc-tagged WT-EGFR was co-expressed with vector-control, FLAG-tagged full-length Ago2 or different domains in 293T cells. Anti-FLAG immunoprecipitates were blotted with myc antibody to show the interaction between EGFR and Ago2. **c,** Pull-down assay was performed by incubating *in vitro* translated full-length EGFR with purified GST-control, GST-Ago2-FDM2, GST-Ago2-FDM4, or GST-full-length-Ago2. Protein samples were precipitated with Glutathione-sepharose beads and subjected to SDS-PAGE, which was visualized by S-35 radioisotopic detection. The quantity of precipitated GST-fusing protein is shown by Coomassie blue staining.

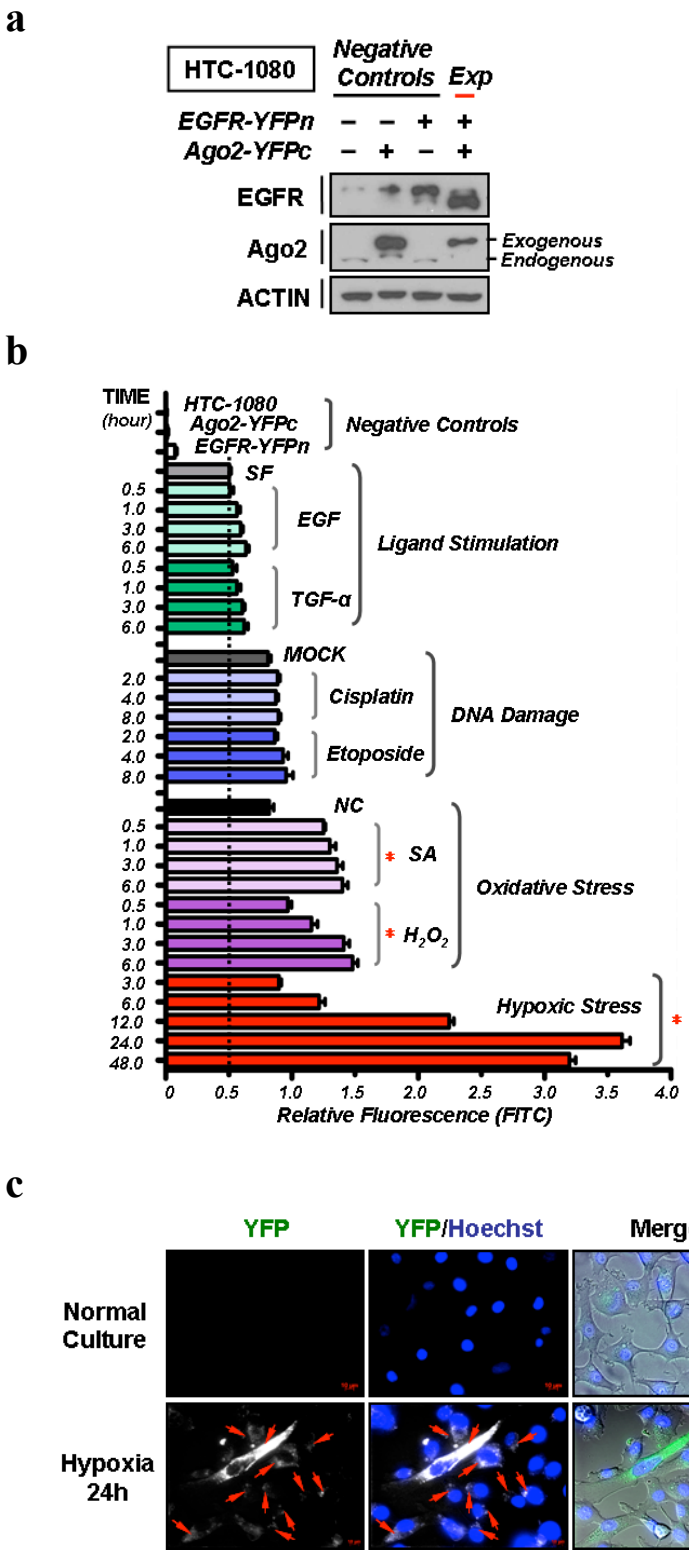

Supplementary Figure 3. EGFR interacts with Ago2 in response to hypoxia and oxidative stress. a, Western blot analysis of total cell lysates from HTC-1080 parental and HTC-1080 stable transfectants expressing Ago2-YFPc, EGFR-YFPn or both EGFR-YFPn and Ago2-YFPc, as indicated. **b,** YFP fluorescence (detected by Flow Cytometry in FITC channel) was induced upon co-expression of EGFR and Ago2, and was further enhanced

when cells were cultured under hypoxia or oxidative stress. SF: Serum-Free O/N; EGF: 20 ng/ml; TGF-α: 10 ng/ml; Cisplatin: 50 μM; Etoposide: 50 μM; SA: Sodium Arsenite (500 μM); H_2O_2: 500 μM; Hypoxia: 1% O_2. Dashed line indicates the basal level of fluorescence detected in serum-starved HTC-1080 stable transfectant co-expressing EGFR and Ago2. All data were normalized to the one of HTC-1080 parental cells (Relative YFP Fluorescence = YFP Fluorescence − Auto-Fluorescence detected in HTC-1080 parental cells) with default setting Auto-Fluorescence =0. Statistical analysis was carried out using student's *t* test. The group of treatment was compared to its corresponding experimental control (ligands vs. SF; Cisplatin and Etoposide vs. MOCK; SA, H_2O_2 and hypoxia vs. NC). Data are shown as mean ± s.d., *n*=3. *indicates P<0.05. **c,** Representative live-cell images showing Hypoxia induced YFP fluorescence in HTC-1080 stable transfectant co-expressing split-half-YFP-tagged EGFR and Ago2. Living cells were stained with Hoechst (marker for nuclear) to show the cytoplasmic localization of the YFP foci as marked by red arrows.

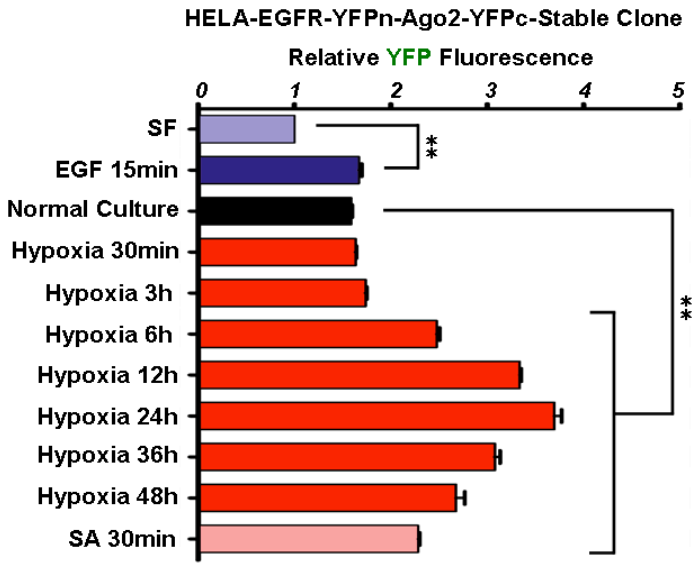

Supplementary Figure 4. EGFR interacts with Ago2 in response to hypoxia and oxidative stress. Similar YFP-interaction system was generated in HeLa cell line. The YFP fluorescence (detected in FITC channel) of HeLa stable transfectant (expressing both EGFR-YFPn and Ago2-YFPc) in response to ligand stimulation (EGF, 20 ng/ml), SA treatment (500 μM) or hypoxia (1% O_2) was analyzed by flow cytometry. All the data were normalized to the basal level of fluorescence in SF (serum-free O/N) group. Statistical analysis was carried out using student's *t* test. Data are shown as mean ± s.d., *n*=3. **indicates P<0.01.

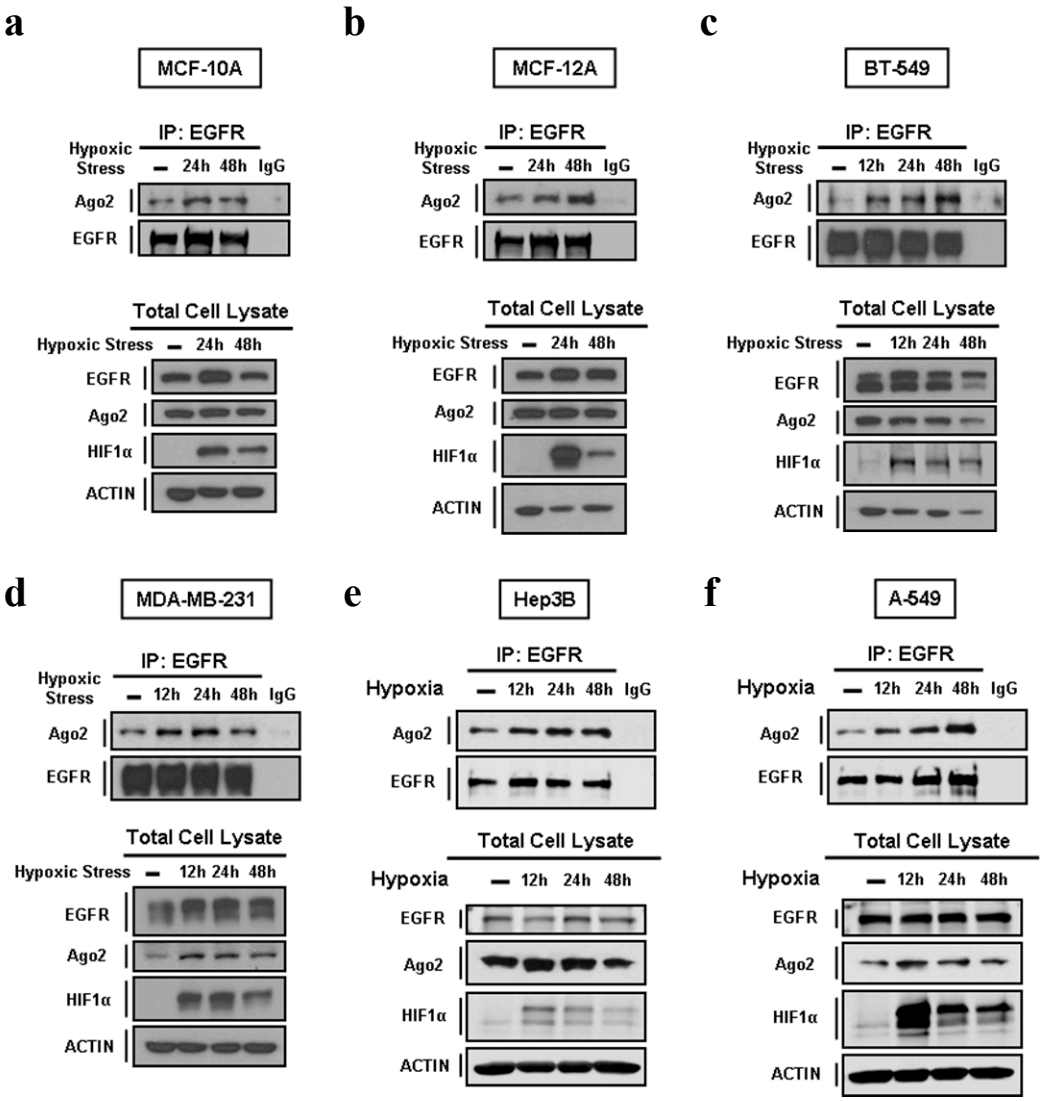

Supplementary Figure 5. EGFR-Ago2 interaction was enhanced by hypoxia in multiple cell lines. Western blot analysis of endogenous EGFR immunoprecipitated from **a,** MCF-10A (breast); **b,** MCF-12A (breast); **c,** BT-549 (breast); **d,** MDA-MB-231 (breast); **e,** Hep3B (liver) and **f,** A-549 (lung) cells cultured under normoxia or hypoxia, as indicated. HIF1α was used as a positive control for cell hypoxic response. β-actin was used as protein loading control.

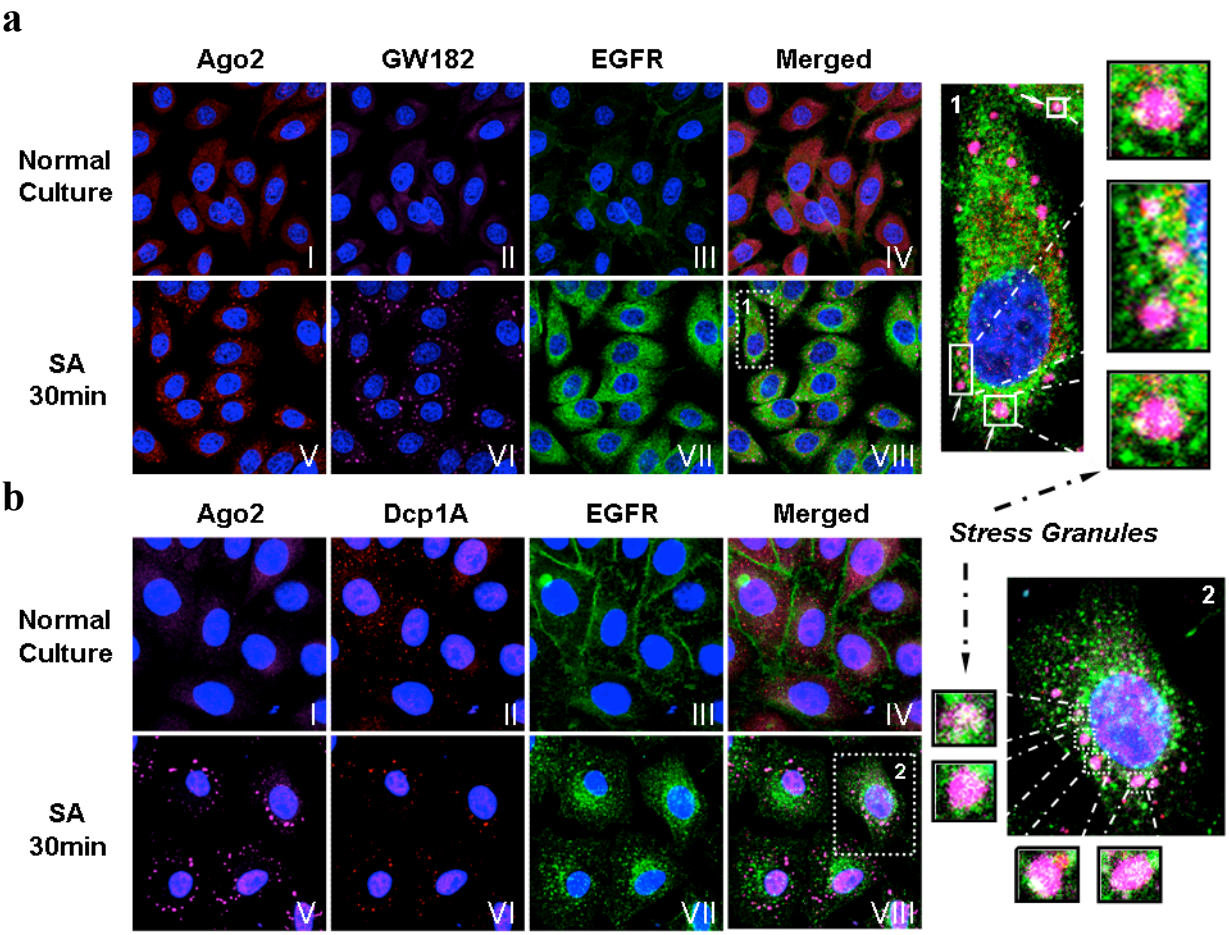

Supplementary Figure 6. EGFR colocalizes with Ago2 in a sub-population of SA-induced stress granules. a, HeLa cells were cultured in normal medium or treated with 500 μM sodium arsenite (SA, classical stress granule inducer) for 30 min. Cells were fixed and stained against endogenous Ago2 (red), GW182 (magenta), EGFR (green) and DAPI (blue). Stress granules are indicated by the SA-induced colocalization of Ago2 and GW182[29]. Right: magnification of image insets. **b,** Left, HeLa cells with same treatments as panel **a** were fixed and stained against endogenous Ago2 (magenta), Dcp1A (red), EGFR (green) and DAPI (blue). Stress granules are indicated by the SA-induced colocalization of Ago2 and Dcp1A[29]. Right, enlargement of the insets.

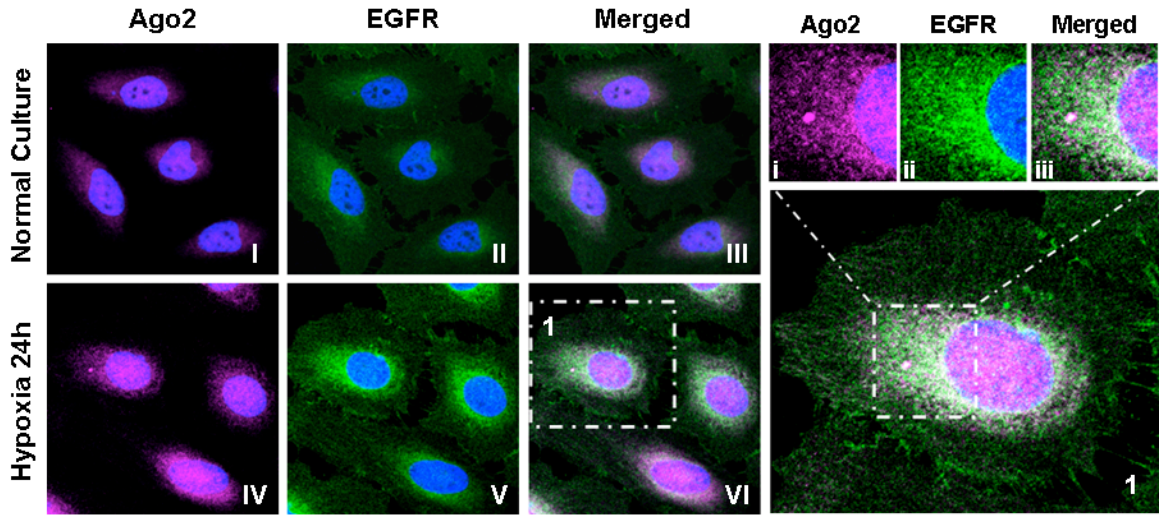

Supplementary Figure 7. EGFR colocalizes with Ago2 in response to hypoxic stress. HeLa cells were cultured under normoxia or hypoxia (1% O_2) for 24 hr. Cells were then fixed and stained against endogenous Ago2 (magenta), EGFR (green) and DAPI (blue). Right: magnification of image insets.

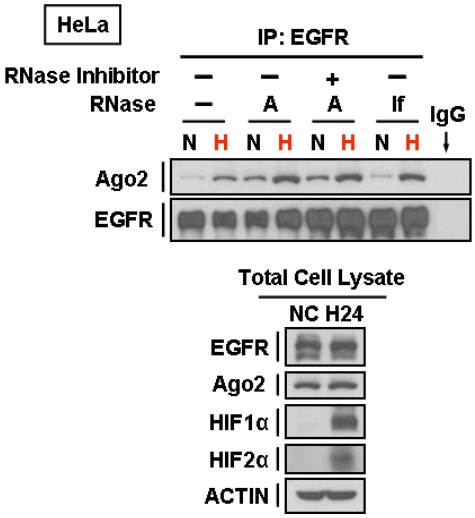

Supplementary Figure 8. Hypoxia-enhanced EGFR-Ago2 interaction is resistant to RNase treatments. Western blot analysis of total cell lysates and EGFR immunoprecipitates from HeLa cells that were cultured under normoxia or hypoxia for 24 hr, as indicated. Cell lysates were treated with 2 μg RNase A (cleaving single-stranded RNA, Sigma) with or without 500 units of ribonuclease inhibitor RNase-Out (Life Technologies) or 100 unites of RNase I_f (single strand specific RNA endonuclease, NEB) as indicated at 4 °C overnight before performing immunoprecipitation. N, normoxia; H, hypoxia for 24 hr.

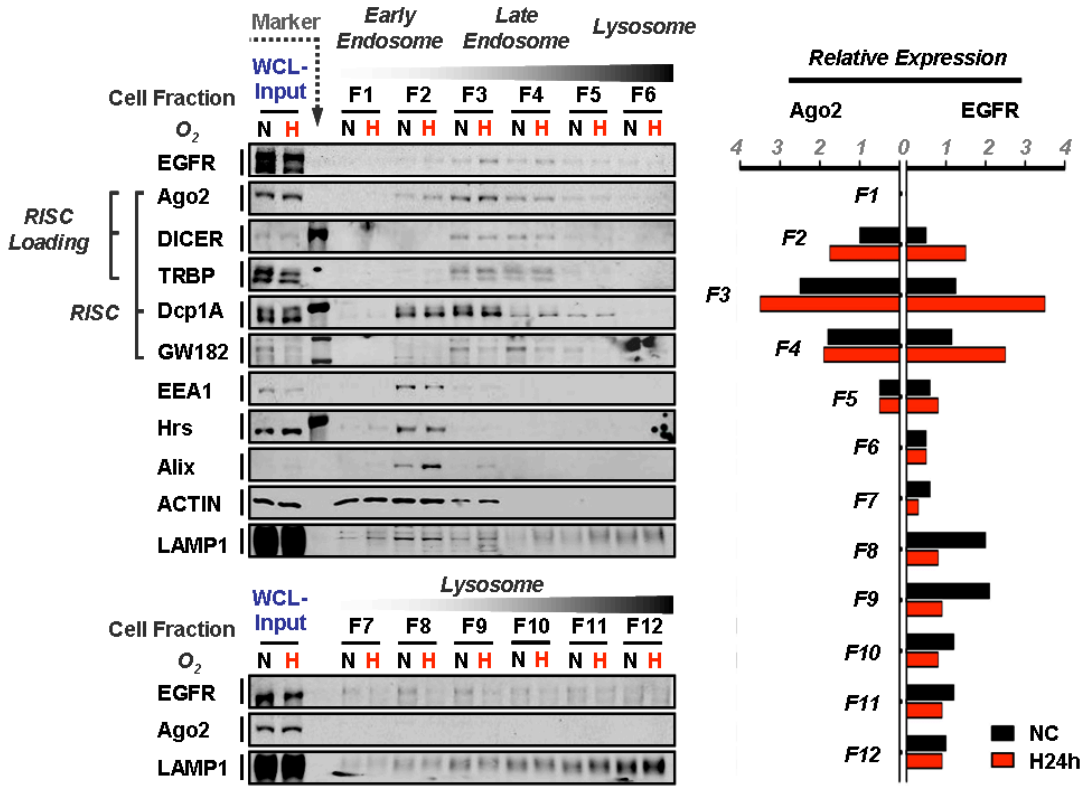

Supplementary Figure 9. EGFR is co-fractionated with RISC loading complex and RISC complex at late endosome/MVB (multivesicular body). Left, Western blot analysis of endogenous EGFR, Ago2, and other known components of RISC[30] and RISC loading complex[10], as indicated, in cell fractions from early endosomes (F1-2, indicated by Actin, EEA1 and Hrs), late endosomes/MVB (F2-4, indicated by Hrs, Alix, Actin and Lamp1), to lysosomes (F4-12, indicated by Lamp1). Ago2 was enriched in late endosomes/multivesicular bodies (MVBs), consistent with previous reports[31,32]. N, cultured under normoxia; H, cultured under hypoxia for 24 hr. Right, relative expression (each fraction signal was normalized according to its corresponding WCL-input) of EGFR and Ago2 in each fraction as indicated.

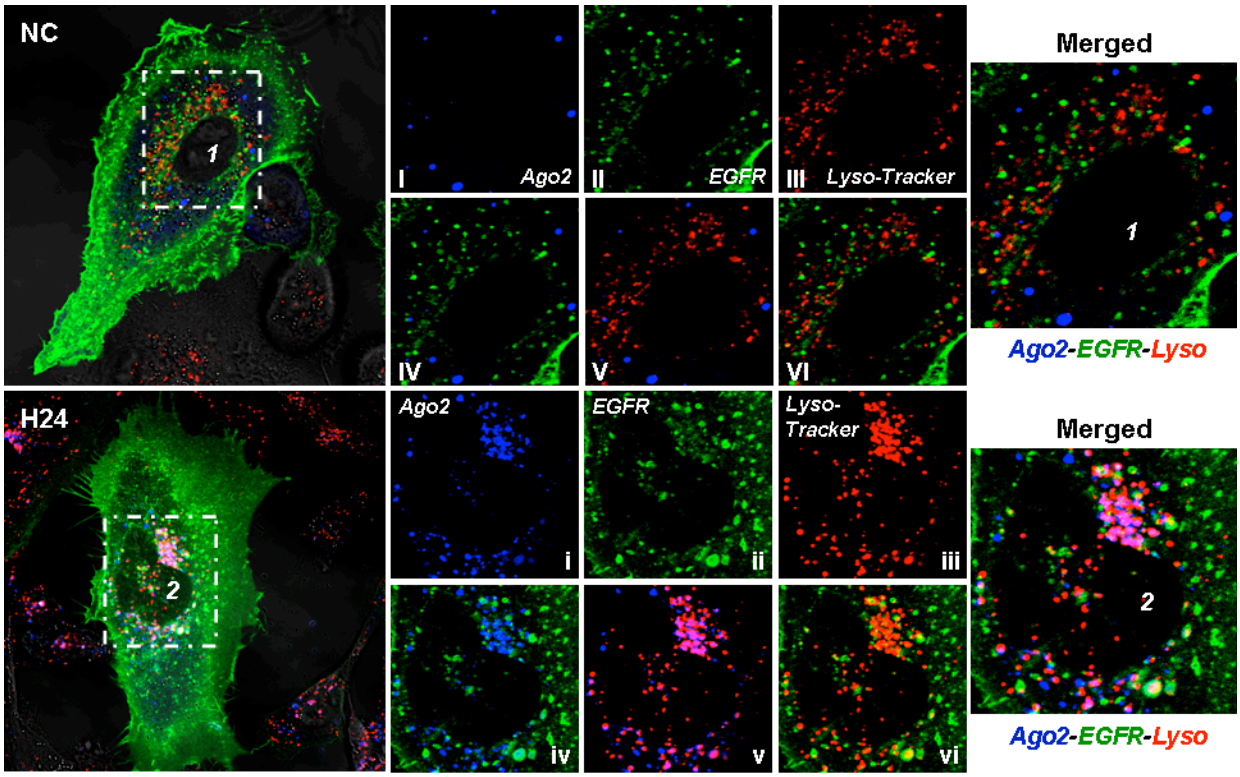

Supplementary Figure 10. EGFR colocalizes with Ago2 at late endosomes/MVBs or lysosomes in response to hypoxia. HeLa cells co-transfected with EGFR-GFP (green) and BFP-Ago2 (blue) were cultured under normoxia or hypoxia (1% O_2) for 24hr. Cells were stained with 50 nM Lyso-Tracker (red color, accumulated in low internal PH compartments[33]) right before live-cell confocal imaging. Hypoxia enhanced colocalization of EGFR and Ago2 at late endosomes/MVBs/lysosomes is indicated by the positive staining of Lyso-Tracker. Right: magnification of image insets.

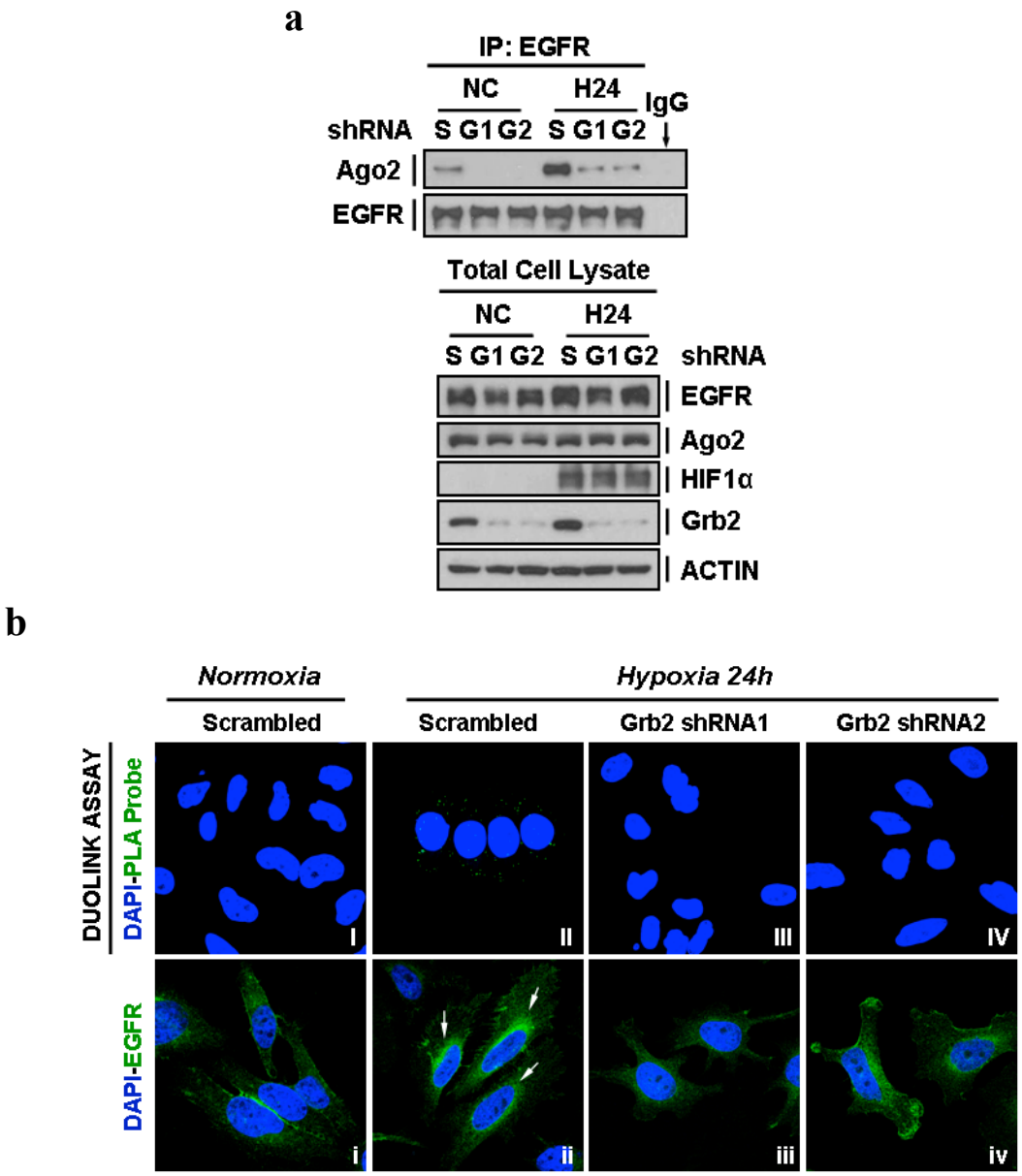

Supplementary Figure 11. Grb2-mediated internalization is critical for the interaction between EGFR and Ago2. a, Western blot analysis of total cell lysates and EGFR immunoprecipitates from HeLa stable transfectants expressing scrambled control or shRNAs targeting Grb2 that were cultured under normoxia or hypoxia for 24 hr as indicated. S, scrambled control; G1, Grb2 shRNA1; G2, Grb2 shRNA2. HIF1α was used as positive control for cell hypoxic response. β-actin was used as protein loading control. **b,** Upper panel, in situ proximity ligation assay was performed in HeLa stable transfectants expressing scrambled control or shRNAs targeting Grb2 that were cultured under normoxia or hypoxia for 24 hr as indicated. Each GFP foci indicated one cluster of EGFR-Ago2 colocalization. Lower panel, HeLa stable transfectants treated the same as upper panel were fixed and stained against endogenous EGFR (green) and DAPI (blue). Hypoxia enhanced EGFR internalization as marked by the arrows in image ii. Grb2 knockdown blocked EGFR endocytosis as expected.

a

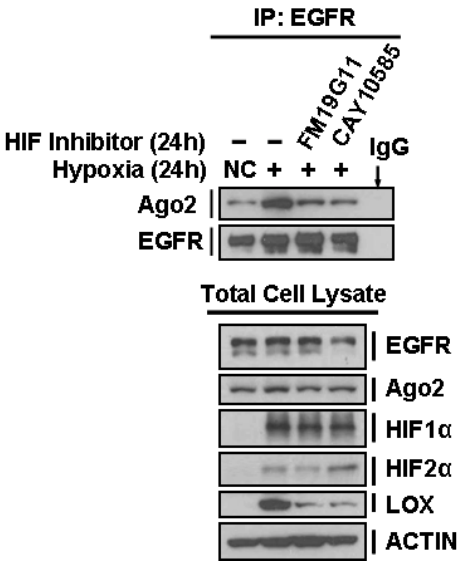
IP: EGFR
FM19G11
CAY10585
HIF Inhibitor (24h) – – IgG
Hypoxia (24h) NC + + +
Ago2
EGFR
Total Cell Lysate
EGFR
Ago2
HIF1α
HIF2α
LOX
ACTIN

b

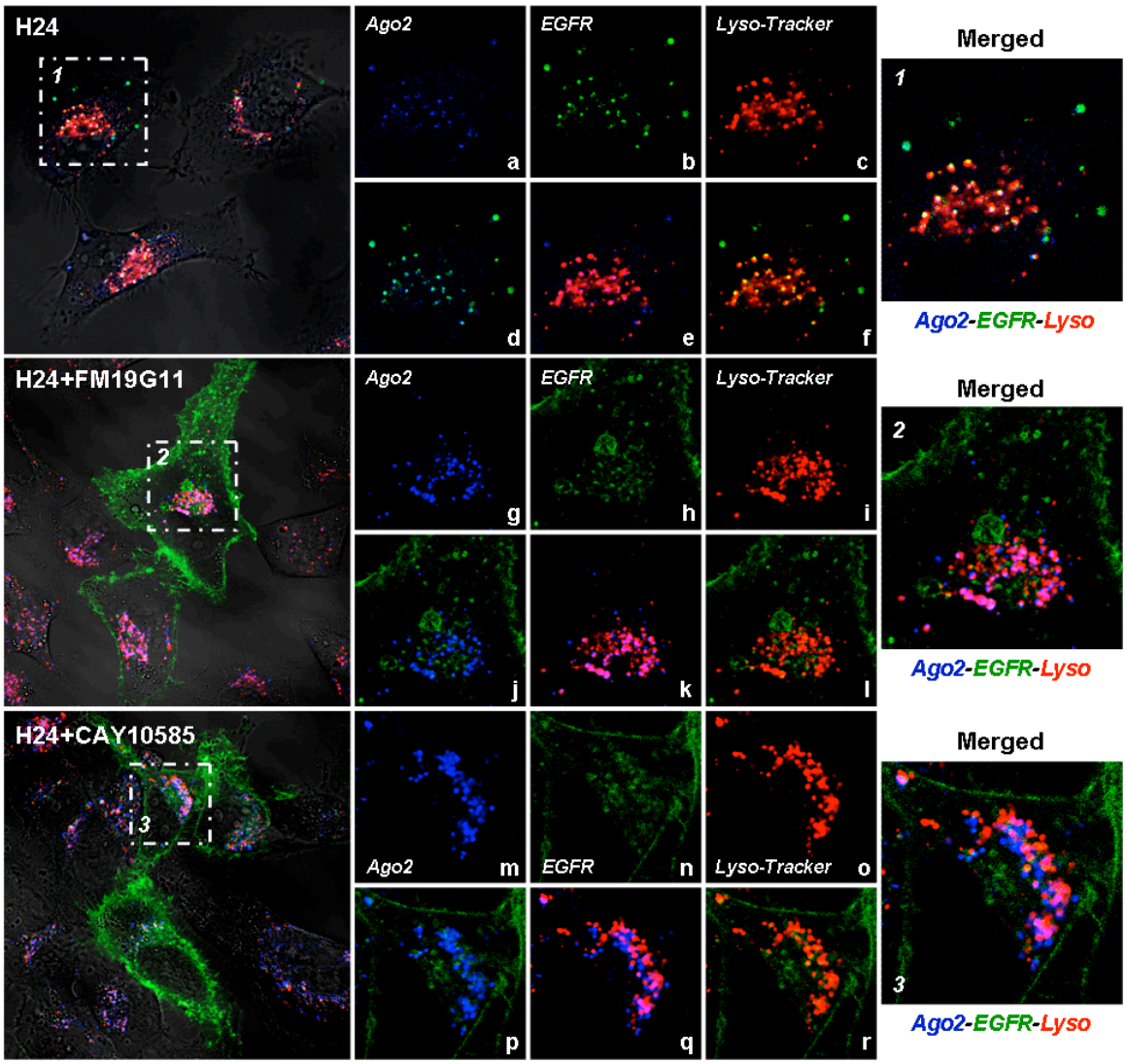
H24
H24+FM19G11
H24+CAY10585
Ago2
EGFR
Lyso-Tracker
Merged
Ago2-EGFR-Lyso

Supplementary Figure 12. The transcriptional activity of HIF1/2α is important for hypoxia-enhanced EGFR-Ago2 interaction. a, Western blot analysis of total cell lysates and EGFR immunoprecipitates from HeLa cells that were cultured under normoxia or hypoxia with or without HIF1/2α inhibitors for 24 hr as indicated. The efficacy of HIF1/2α inhibitors was reflected by the reduced expression of LOX, a well-known target of HIF1/2α[34]. HIF1/2α as used as positive control for cell hypoxic response. β-actin was used as protein loading control. **b,** HeLa cells co-transfected with EGFR-GFP (green) and BFP-Ago2 (blue) were cultured under hypoxia (1% O_2) with or without HIF1/2α inhibitors (FM19G11 inhibits the transcriptional activity of HIF1/2α[35]; CAY10585 blocks HIF1α accumulation and reduces its transcriptional activity[36]) for 24hr. Cells were stained with 50 nM Lyso-Tracker (red color, accumulated in low internal PH compartments) right before live-cell confocal imaging. Right: magnification of image insets.

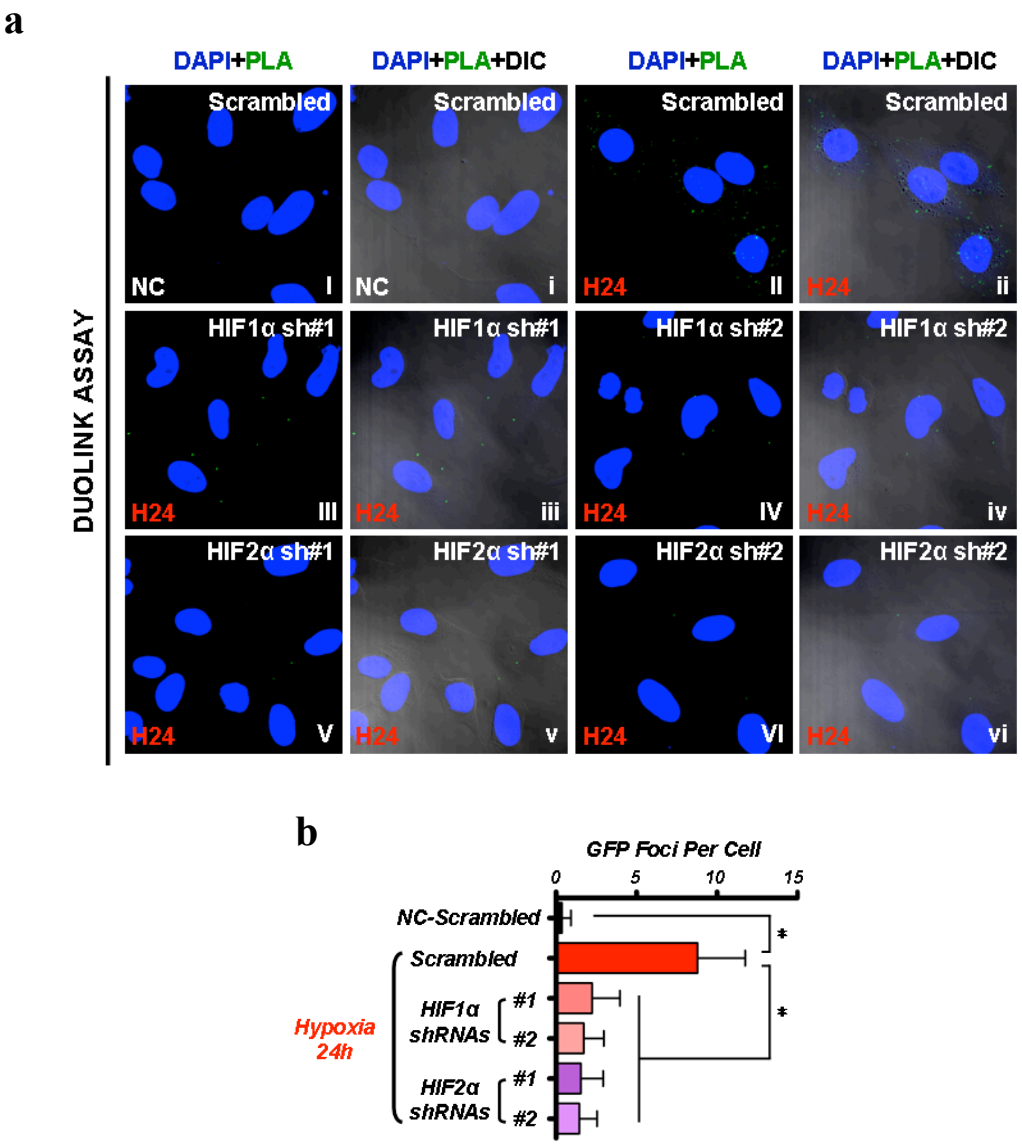

Supplementary Figure 13. Both HIF1α and HIF2α are important for EGFR-Ago2 interaction in response to hypoxia. a, *In situ* proximity ligation assay was performed in HeLa stable transfectants expressing scrambled control or shRNAs targeting HIF1α or HIF2α as indicated that were cultured under normoxia or hypoxia for 24 hr. Each GFP foci indicated one cluster of EGFR-Ago2 colocalization/interaction. **b,** Quantitative result for panel **a**. Fifty cells in each experimental group were counted for the number of GFP foci per cell. Statistical analysis was carried out using student's *t* test. HIF1/2α knockdown cells were treated as one group to compare with the scrambled control. Data are shown as mean ± s.d., *n*=50. *indicates P<0.05.

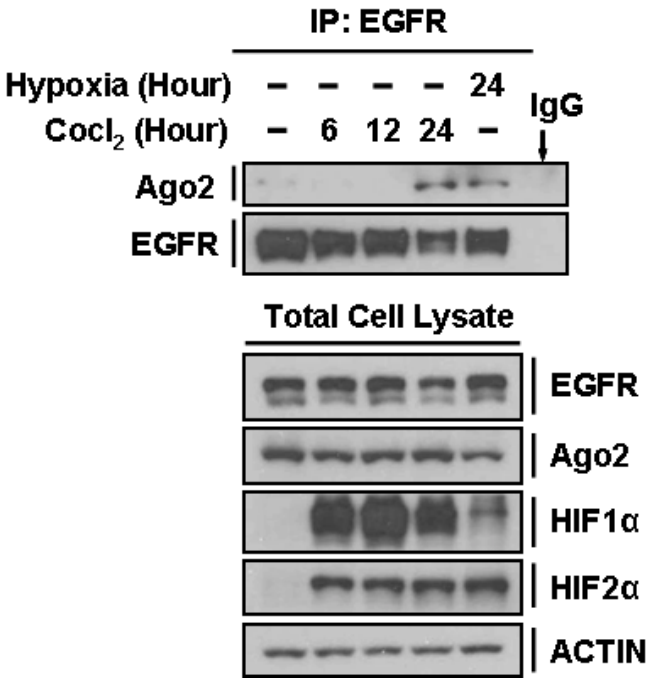

Supplementary Figure 14. Stabilization of HIF1/2α by $CoCl_2$ treatment finally enhanced EGFR-Ago2 interaction under normoxia. Western blot analysis of the total cell lysates and EGFR immunoprecipitates from HeLa cells that were treated with $CoCl_2$ (100 μM) or cultured under hypoxia for 24 hr as indicated. The expression of HIF1/2α was stabilized right after $CoCl_2$ treatment for 6 hr (consistent with previous report[37]), whereas the interaction between EGFR and Ago2 was not induced until 24 hr later (similar to what we found in EGFR-Ago2 association in response to hypoxia), suggesting that downstream events of HIF1/2α stabilization may also play a role in EGFR-Ago2 interaction.

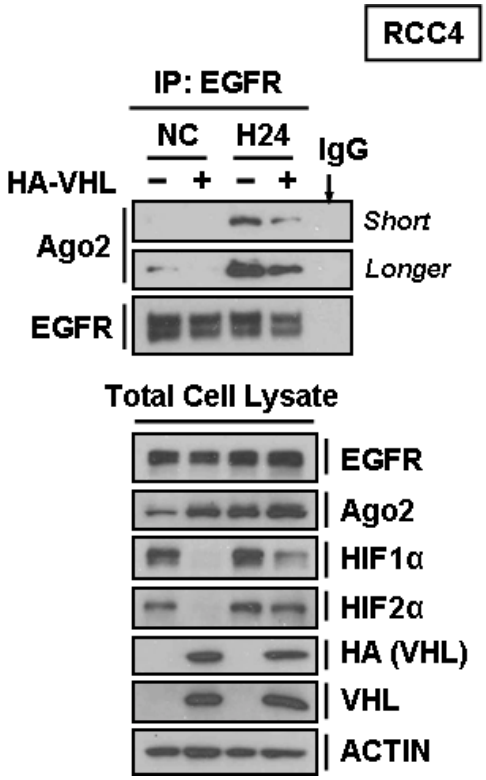

Supplementary Figure 15. EGFR-Ago2 interaction was induced by hypoxia through HIF1/2α dependent and independent mechanisms. Western blot analysis of the total cell lysates and EGFR immunoprecipitates from RCC4 (endogenous VHL null with constitutively expressed HIF1/2α) stable transfectants expressing vector control or WT-VHL that were cultured under normoxia or hypoxia for 24 hr. Re-expression of WT-VHL in RCC4 cells reduced the expression of HIF1/2α as previously reported[38] and decreased the association between EGFR and Ago2. However, EGFR-Ago2 interaction in RCC4 vector control and WT-VHL stable clones was further induced by hypoxia regardless of the constitutively expressed HIF1/2α.

a

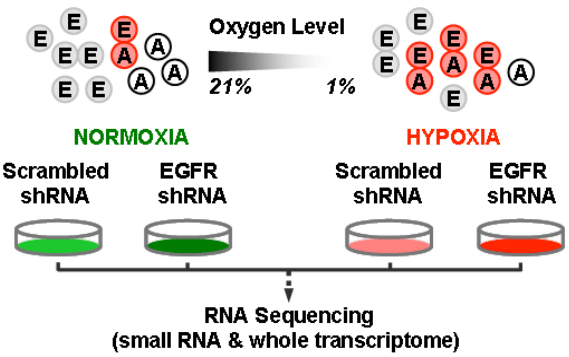

b

Define R-Pre and R-Mature:
Relative Expression Affected by EGFR

R-Pre = Log_2 Pre-miR (Scrambled) - Log_2 Pre-miR (EGFR shRNA-E1)
R-Mature = Log_2 Mature-miR (Scrambled) - Log_2 Mature-miR (EGFR shRNA-E1)

Supplementary Figure 16. Experimental design for RNA deep sequencing analysis. a, Total RNA extracted from HeLa stable clones expressing scrambled control or EGFR shRNA (shRNA-E1) that cultured under normoxia or hypoxia for 24 hr was analyzed by RNA deep sequencing for both small RNA application and whole transcriptome analysis. E, EGFR; A, Ago2. Red circles indicate the interaction between EGFR and Ago2. **b,** Definition of R-Pre and R-Mature for Hierarchical Clustering Analysis.

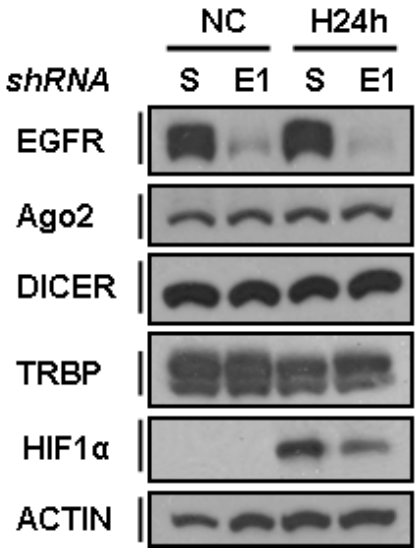

Supplementary Figure 17. Verification of EGFR knockdown efficacy in HeLa stable transfectants for RNA deep sequencing. Western blot analysis of total cell lysates from HeLa stable clones expressing scrambled control or EGFR shRNA-E1 that were cultured under normoxia or hypoxia for 24 hr. HIF1α was used as a positive control for cell hypoxic response. β-actin was used as protein loading control. S, scrambled control; E1, EGFR shRNA-E1.

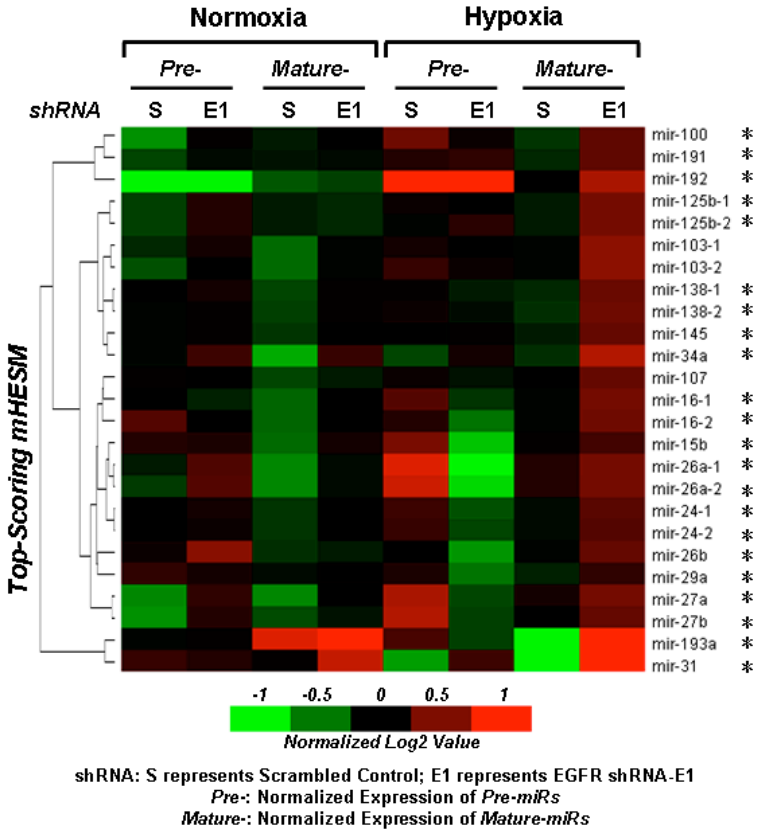

Supplementary Figure 18. Hierarchical Clustering Analysis of top-scoring mHESM. mHESMs were sorted based on their absolute mature miRNA expression affected by EGFR knockdown. 20 top-scoring mHESM were selected (note: miR-193a includes miR-193a-5p and miR-193a-3p) and tumor-suppressor-like miRNAs were marked with an asterisk (*). Expression of pre- or mature miRNAs was log2 transformed and further normalized by mean centering to correct average gene expression from all the samples as log2-ratio of 0. Centroid Linkage Clustering was performed and the interactive graphical result from Cluster was analyzed by TreeView to display the heatmap.

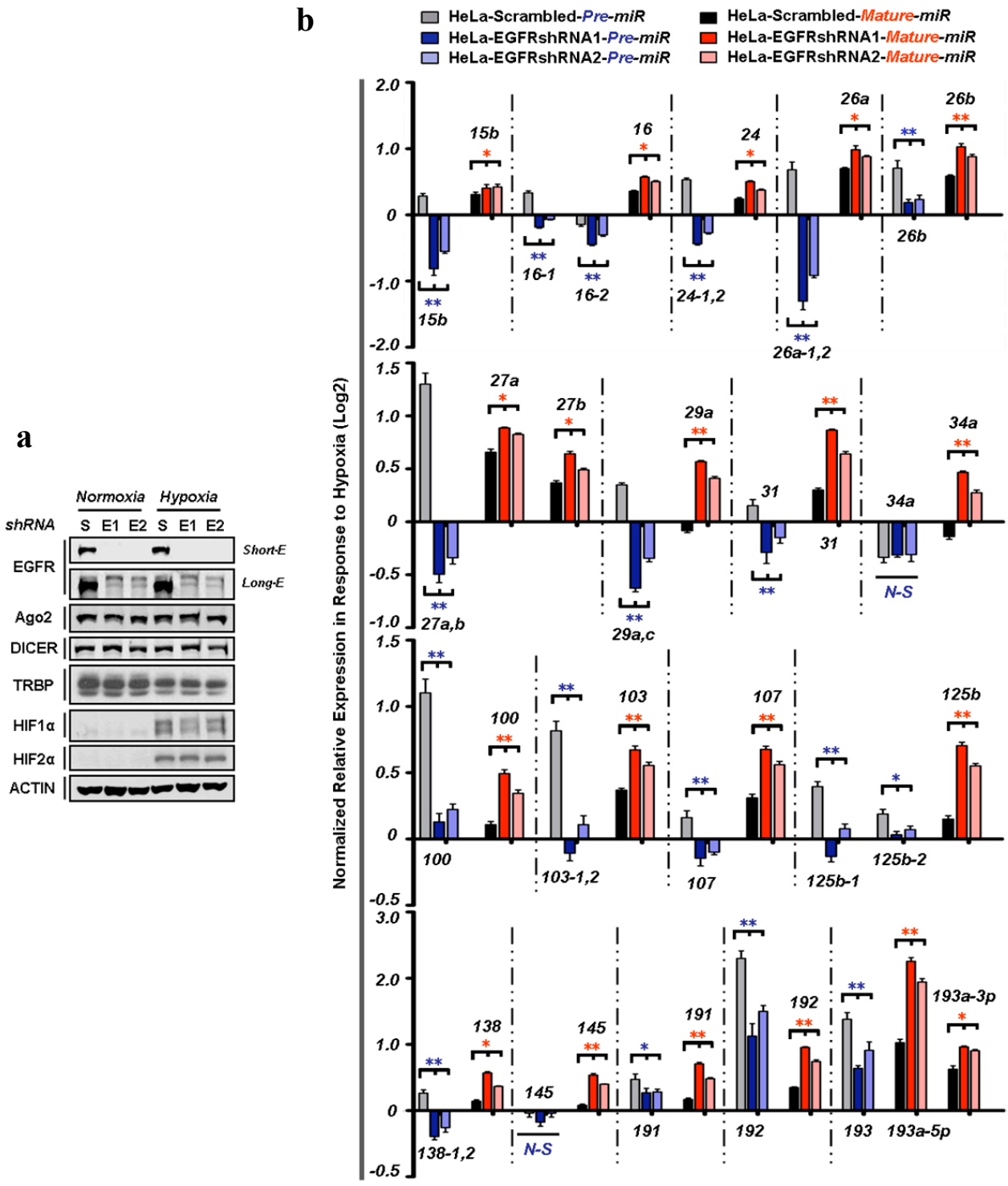

Supplementary Figure 19. EGFR suppresses the maturation of mHESM in response to hypoxia. a, Western blot analysis of HeLa stable clones expressing scrambled control or EGFR shRNAs (E1, E2) that cultured under normoxia or hypoxia for 24 hr, as indicated. S, scrambled control; E1, EGFR shRNA-E1; E2, EGFR shRNA-E2. HIF1α and HIF2α were used as positive control for cell hypoxic response. β-actin was used as protein loading control.

b, Normalized relative expression (Log2) of pre- and mature miRNAs in HeLa stable clones (verified in panel **a**) in response to hypoxia. Statistical analysis was carried out using Student's *t* test. EGFR knockdown cells (E1 and E2) were considered as one group to compare with the scrambled control. Data are shown as mean ± s.d., *n*=4, *N-S* indicates P>0.05, * indicates P<0.05, **indicates P<0.01.

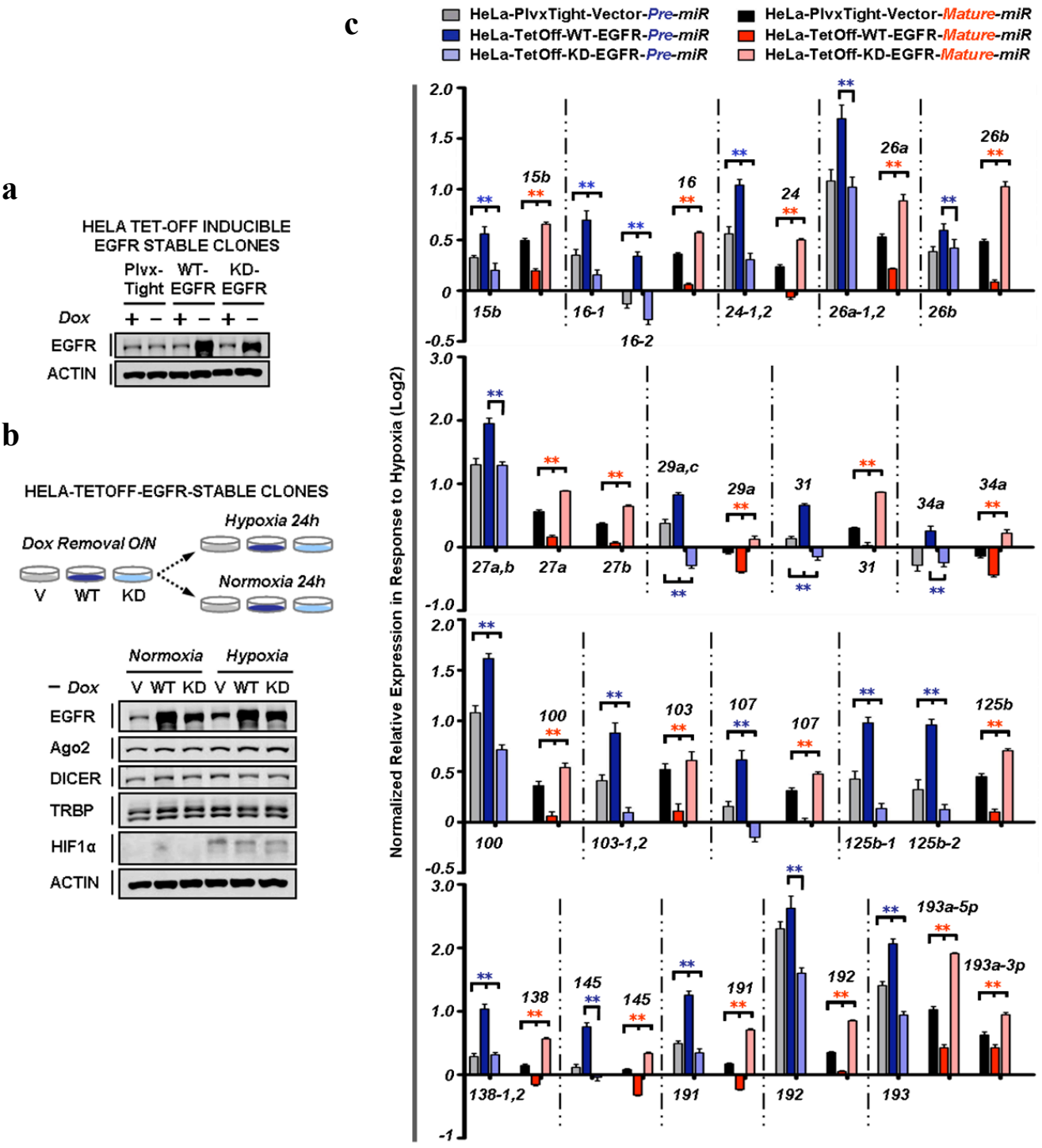

Supplementary Figure 20. EGFR kinase activity is essential for EGFR-suppressed miRNA maturation. a, HeLa TetOff-inducible stable clones expressing vector control, wild-type (WT) or kinase-dead (KD) EGFR were generated and validated by Western blot. **b,** Western blot analysis of HeLa TetOff-inducible EGFR stable clones that cultured under normoxia or hypoxia for 24 hr after doxycycline removal O/N. HIF1α was used as positive control for cell hypoxic response. β-actin was used as protein loading control. **c,** Normalized

relative expression (Log2) of pre- and mature miRNAs in HeLa TetOff-inducible EGFR stable clones (verified in panel **b**) in response to hypoxia. Statistical analysis was carried out using ANOVA or student's *t* test (comparing WT and KD EGFR). Data are shown as mean ± s.d., *n*=4. **indicates P<0.01.

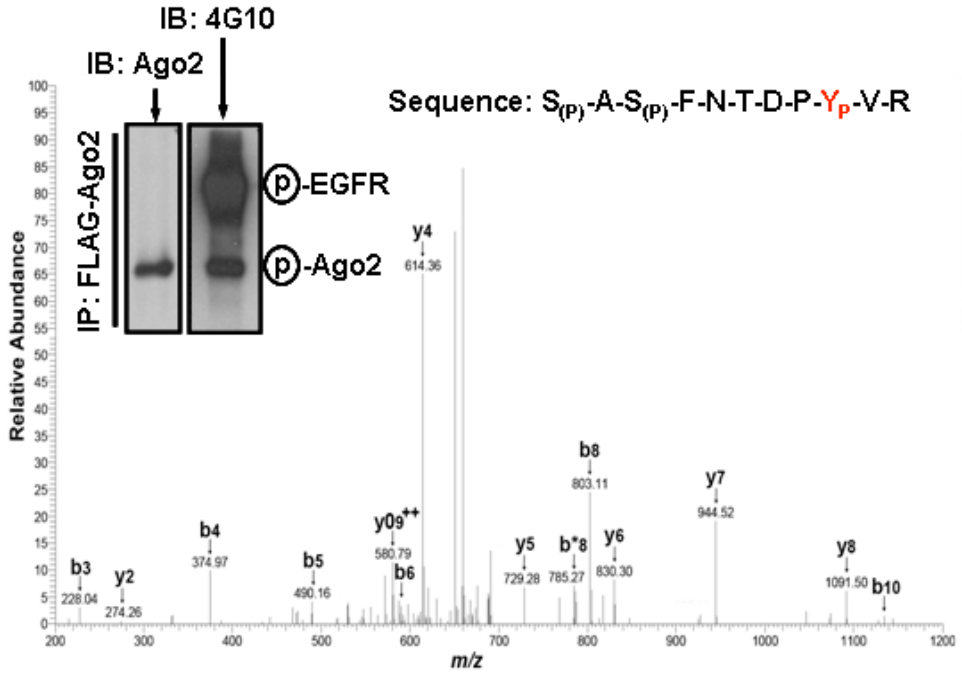

Supplementary Figure 21. Ago2 is tyrosine phosphorylated at residue 393 as identified by mass spectrometric analysis. Top left, Western blot verification showing the tyrosine phosphorylation of purified Ago2 that co-expressed with EGFR in 293T cells. Tyrosine phosphorylation was detected by 4G10 antibody. Bottom, mass spectrometric analysis of Ago2 identified Tyr393 as the single tyrosine residue that been phosphorylated *in vivo*. This phospho-tyrosine residue has previously been reported[39], but neither the enzyme required for this phosphorylation nor the biological outcomes of Ago2-Y393 phosphorylation has been studied so far.

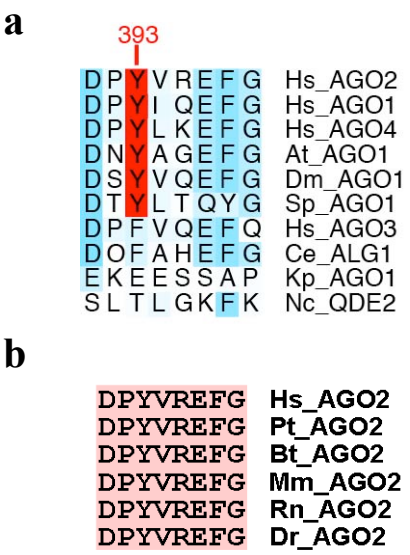

Supplementary Figure 22. Tyr393 of hAgo2 is highly conserved among vertebrates and coexists in hAgo1, hAgo4 but not hAgo3. a, Sequence alignment of the AGO family around Y393 of hAgo2. Highlighted with blue are well-conserved amino acids (intensity indicates degree of conservation). Hs, *Homo sapiens*; At, *Arabidopsis thaliana*; Dm, *Drosophila melanogaster*; Sp, *Saccharomyces pombe*; Ce, *Caenorhabditis elegans*; Kp, *Kluyveromyces polysporus*; Nc, *Neurospora crassa*. **b,** The adjacent amino acid sequence of hAgo2-Y393 (DPYVREFG) is identical among vertebrates. Hs, *Homo sapiens*; Pt, *Pan troglodytes; Bt, Bos taurus; Mm, Mus musculus; Rn, Rattus norvegicus; Dr, Danio rerio.*

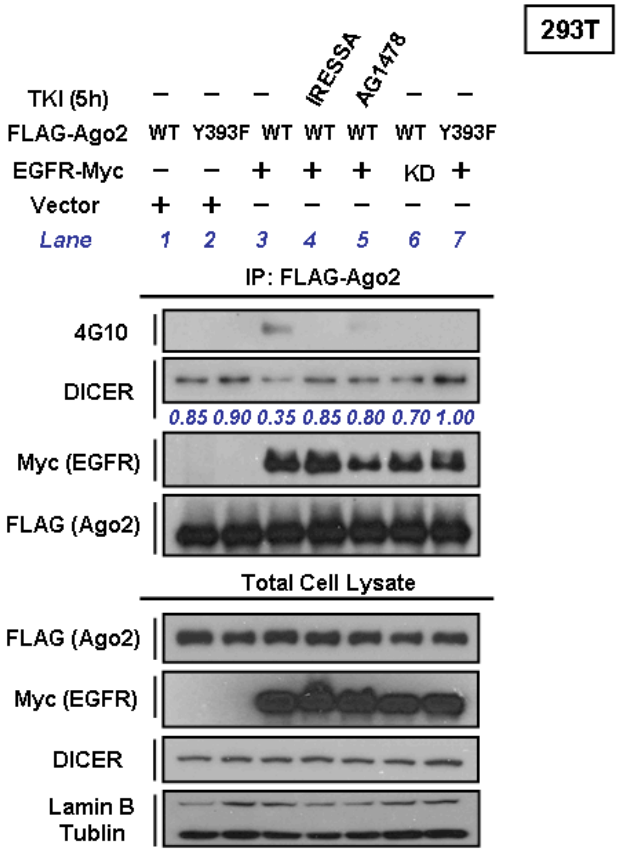

Supplementary Figure 23. Tyr393 of Ago2 is the major phosphorylation site targeted by EGFR *in vivo* and the phosphorylation of this residue reduces Ago2 binding to Dicer. IP-Western analysis of WT and Y393F Ago2 in 293T cells, as indicated. Expression of Y393F mutant Ago2 or treatment with tyrosine kinase inhibitor (TKI) of EGFR abolished EGFR-mediated tyrosine phosphorylation of Ago2 (Lanes 4, 5, 6, 7 vs. Lane 3), supporting this residue as a target of EGFR. Interestingly, phosphorylation of Ago2 at Y393 reduced its interaction with Dicer, which can be restored by either TKI treatment (Iressa or AG1478) or by expressing the Y393F mutant Ago2 (Lane 3 vs. the other lanes). The quantitation of Dicer that interacts with Ago2 is shown below. Iressa (1 μM), tyrosine kinase inhibitor (also known as gefitinib) used in clinic for targeting EGFR; AG1478 (50 nM), specific EGFR inhibitor[40] (IC_{50} for selective inhibition of EGFR = 3 nM *in vitro* vs. IC_{50} for targeting HER2-neu and PDGFR >100 μM).

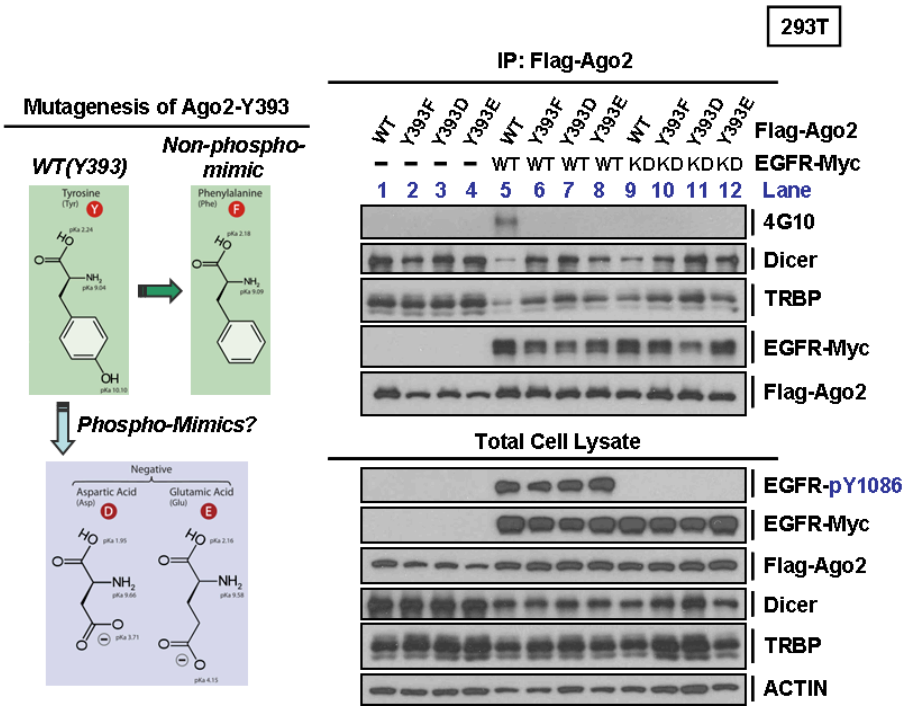

Supplementary Figure 24. Ago2-Y393 phosphorylation reduces Ago2-Dicer/TRBP interaction, which however cannot be imitated by Y393D or Y393E mutant Ago2. Left, Ago2 Y393 was mutated to phospho- and non-phospho-mimics. Right, IP-Western analysis of WT, Y393F, Y393D and Y393E Ago2 in 293T cells, as indicated. WT Ago2 was tyrosine phosphorylated by WT but not KD EGFR (Lane 5 vs. Lane 9). Mutating Tyr393 into phenylalanine (F) or aspartic acid (Y393D) or glutamic acid (Y393E) abolished EGFR mediated tyrosine phosphorylation of Ago2 (Lanes 6, 7, 8 vs. Lane 5). Ago2-Y393 phosphorylation reduced its binding with Dicer and TRBP (Lane 5 vs. Lanes 1, 2, 6, 9, 10). Y393D and Y393E mutants showed similar property as Y393F mutant, suggesting that both aspartic acid and glutamic acid cannot fully imitate phosphorylated Y393 in Ago2. The phenomenon that phospho-tyrosine cannot be mimicked by aspartic acid and glutamic acid was also reported previously (Nicholas J. Anthis et al. Biochem J. 2009)[41].

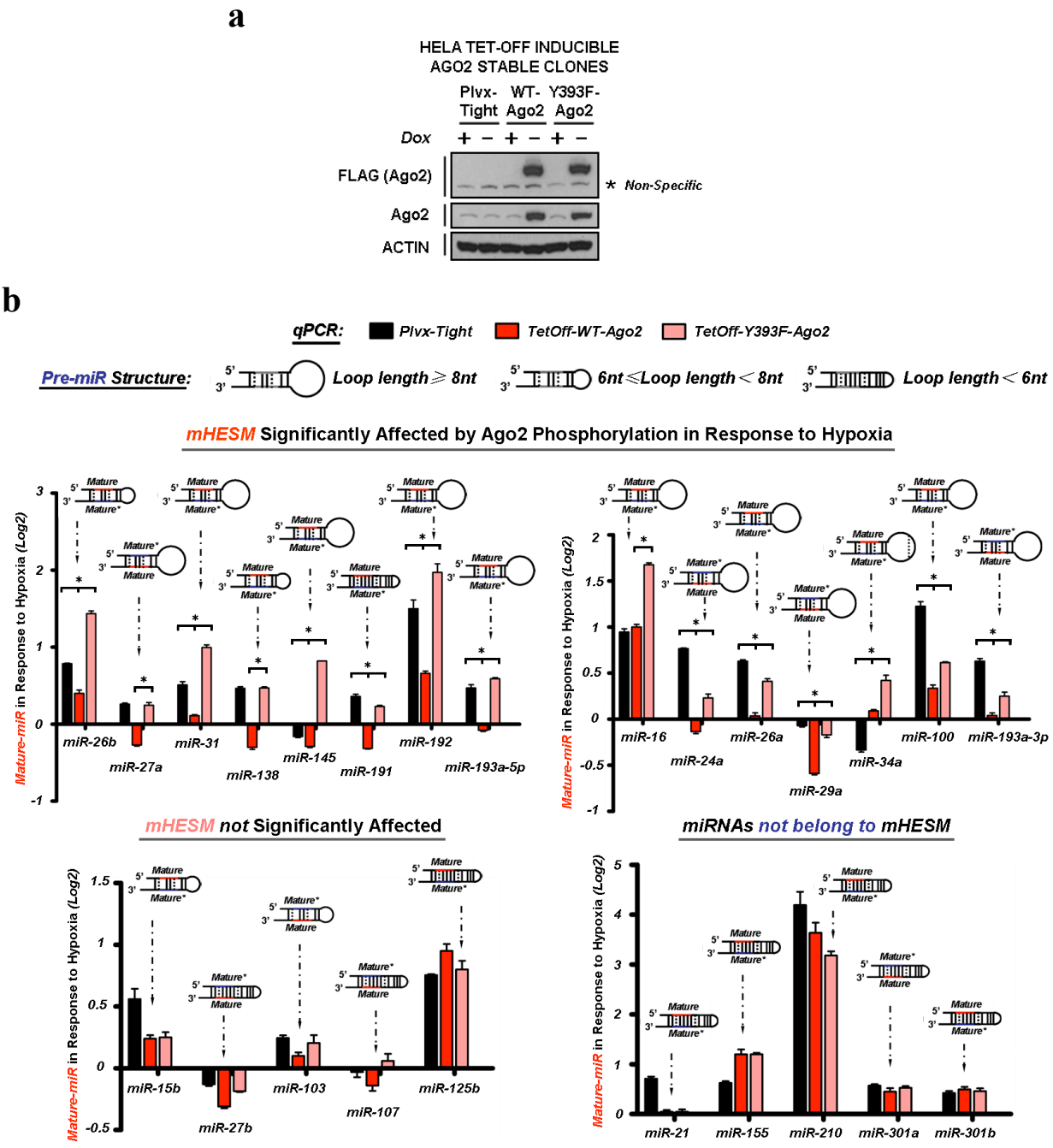

Supplementary Figure 25. Most mHESM regulated by Ago2-Y393 phosphorylation in response to hypoxia contain long-loop structure in their precursors. a, HeLa TetOff-inducible stable clones expressing vector control, WT or Y393F Ago2 were generated and verified by Western blot, as indicated. * indicates the non-specific signal recognized by FLAG antibody. **b,** Normalized relative expression (Log2) of mature miRNAs in HeLa TetOff-inducible Ago2 stable clones (as verified in Fig. 3b) in response to hypoxia. The structures of corresponding miRNA precursors were shown in the diagram. Statistical analysis was carried out using student's *t* test (comparing WT Ago2 or vector control to Y393F Ago2). Data are shown as mean ± s.d., *n*=4, *indicates P<0.05.

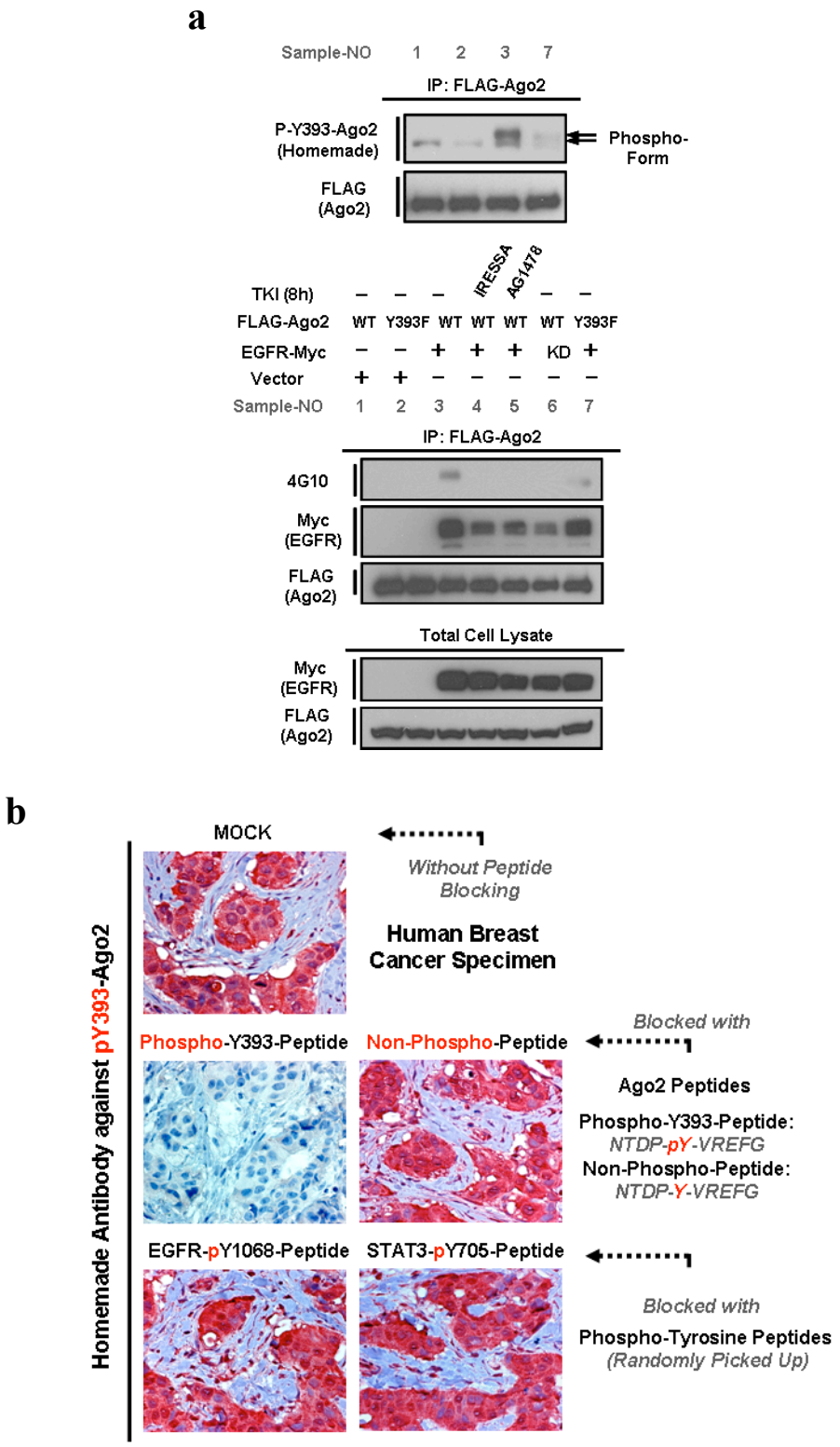

Supplementary Figure 26. Characterization of mouse polyclonal antibody against phospho-Y393-Ago2 (homemade). a, Top, anti-FLAG immunoprecipitates (Sample-NO.1, 2, 3, 7) were blotted with homemade antibody against p-Y393-Ago2. Bottom, Western blot analysis of corresponding anti-FLAG immunoprecipitates and total cell lysates from 293T cells. **b,** Peptide competition assay for p-Y393-Ago2 antibody by immunohistochemical

staining. Human breast tumor sample showing high expression of EGFR (data not shown) also showed positively staining of p-Y393-Ago2 using the homemade antibody. Importantly, the recognition capacity of this antibody can be completely blocked with phospho-Y393-Ago2-peptide but not the control non-phospho-Ago2-peptide or the other randomly chosen phospho-tyrosine peptides, demonstrating its fidelity in IHC staining for detecting Ago2-Y393 phosphorylation *in vivo*.

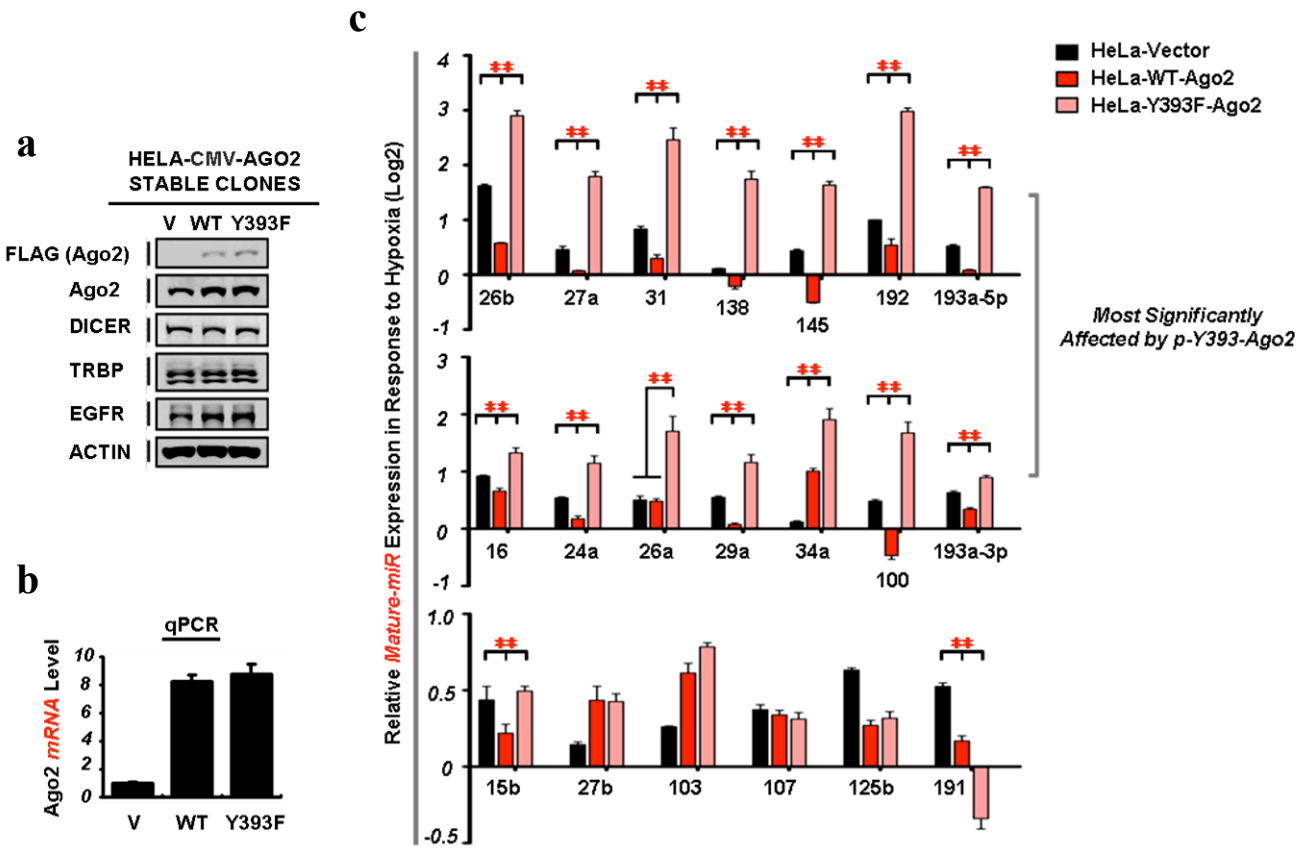

Supplementary Figure 27. Ago2-Y393 phosphorylation reduces the production of most mHESM in HeLa non-inducible stable transfectants in response to hypoxia. a, Western blot verification for non-inducible Ago2 stable clones generated in HeLa cell line, as indicated. **b,** qPCR verification for the mRNA expression of WT and Y393F Ago2 in HeLa non-inducible stable transfectants. β-actin mRNA was used as internal control. **c,** Normalized relative expression (Log2) of mature mHESM in HeLa non-inducible Ago2 stable clones, as verified in panels **a** and **b**, in response to hypoxia. Statistical analysis was carried out using student's *t* test (comparing WT- and Mut-Ago2). Data are shown as mean ± s.d., *n*=4, **indicates P<0.01.

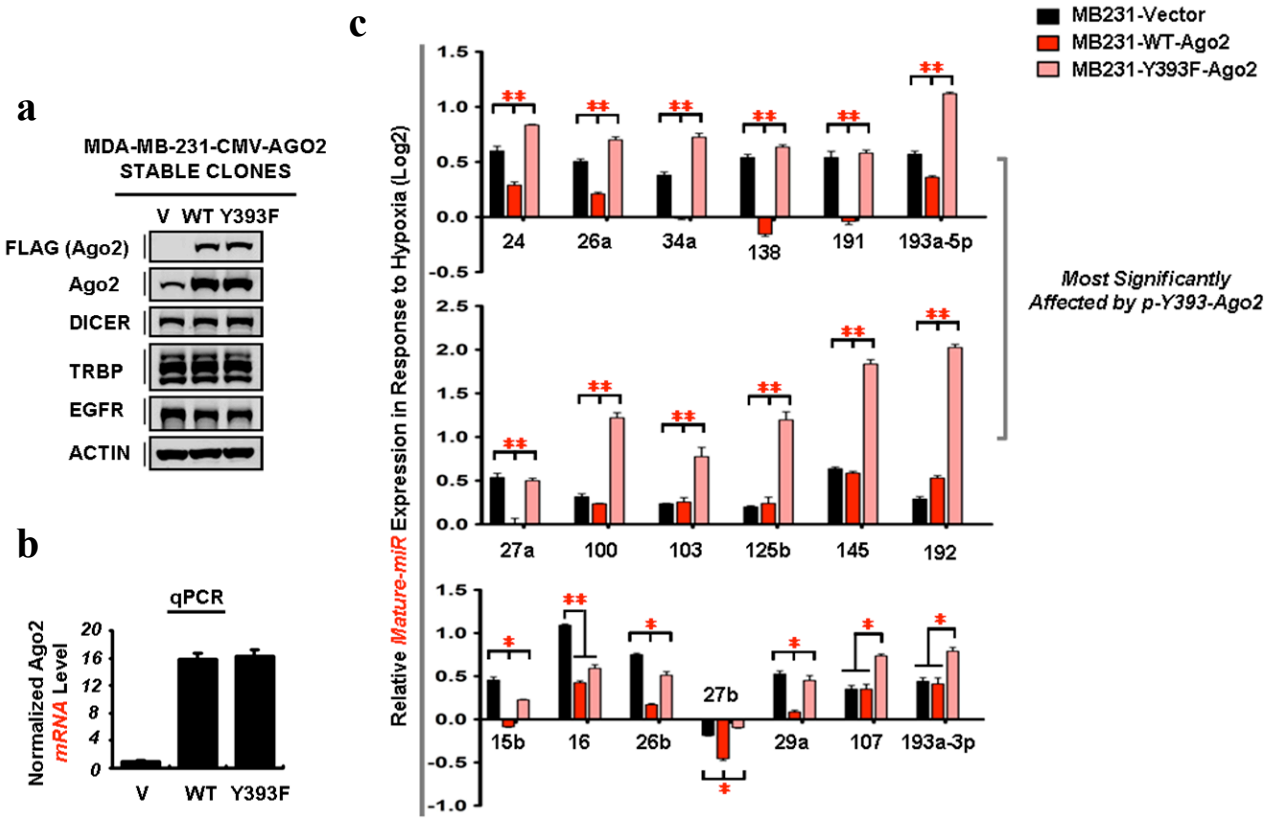

Supplementary Figure 28. Ago2-Y393 phosphorylation suppresses the production of most mHESM in MDA-MB-231 stable transfectants in response to hypoxia. a, Western blot verification for Ago2 stable clones generated in MDA-MB-231 cell line, as indicated. **b,** qPCR verification for the mRNA expression of WT and Y393F Ago2 in MDA-MB-231 stable transfectants. β-actin mRNA was used as internal control. **c,** Normalized relative expression (Log2) of mature mHESM in MDA-MB-231 Ago2 stable clones, as verified in panels **a** and **b**, in response to hypoxia. Note: miR-31 was not expressed in MDA-MB-231 cell line. Statistical analysis was carried out using student's *t* test (comparing WT and Y393F Ago2). Data are shown as mean ± s.d., *n*=4, *indicates P<0.05, **indicates P<0.01.

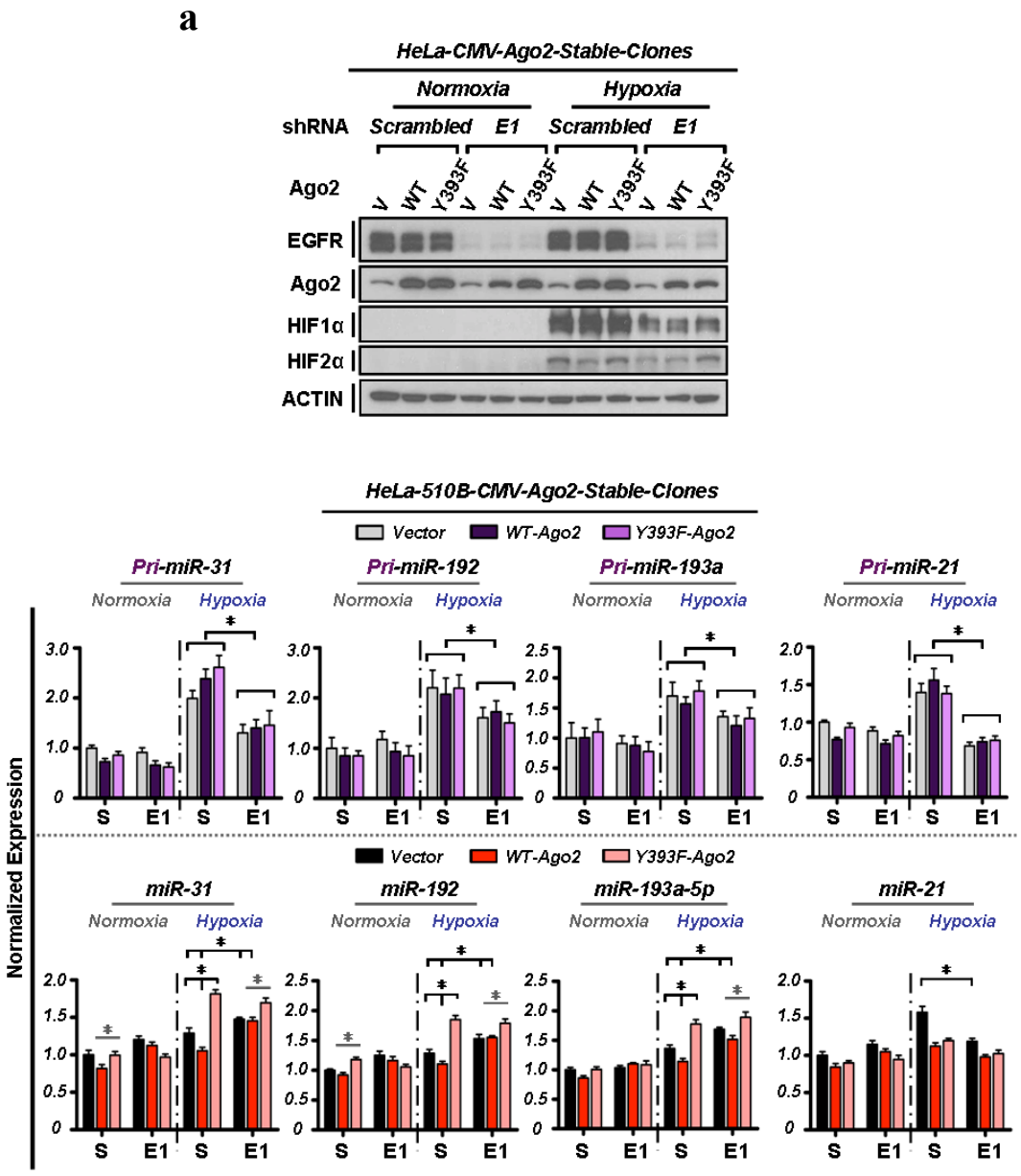

Supplementary Figure 29. EGFR is the tyrosine kinase that suppresses the processing of long-loop mHESM through phosphorylation of Ago2 at Y393 in response to hypoxia. a, Western blot analysis of HeLa CMV Ago2 stable clones expressing scrambled control or EGFR shRNA-E1 that cultured under normoxia or hypoxia for 24 hr. HIF1α and HIF2α were used as positive control for cell hypoxic response. β-actin was used as protein loading control. **b,** Top, normalized expression of pri-miRNAs in HeLa CMV Ago2 stable clones expressing scrambled control or EGFR shRNA-E1, as verified in panel **a**, in response to hypoxia. Bottom, corresponding normalized expression of mature miR-31, miR-192, miR-193a-5p (long-loop mHESM) and miR-21 (non-mHESM). Silencing EGFR suppressed the expression of pri-miR-31, pri-miR-192 and pri-miR-193a (long-loop mHESM representatives) to a similar level among those stable transfectants under hypoxia; however, it enhanced the level of corresponding mature miRNAs in vector control and WT but not Y393F Ago2 cells. The expression of pri- and mature miR-21 (non-mHESM) was decreased by EGFR knockdown,

but was similar between WT and Y393F Ago2 stable clones. These results indicate that increased expression of mature long-loop mHESM in vector control and WT Ago2 cells after EGFR knockdown was not caused by transcriptional upregulation but instead de-repression of miRNA maturation. S, scrambled control; E1, EGFR shRNA-E1. Statistical analysis was carried out using Student's *t* test and the significance shown in the diagram was based on the difference between vector control or WT and Y393F Ago2, or between scrambled control and EGFR knockdown groups, as indicated. Data are shown as mean ± s.d., n=4, * indicates $P<0.05$.

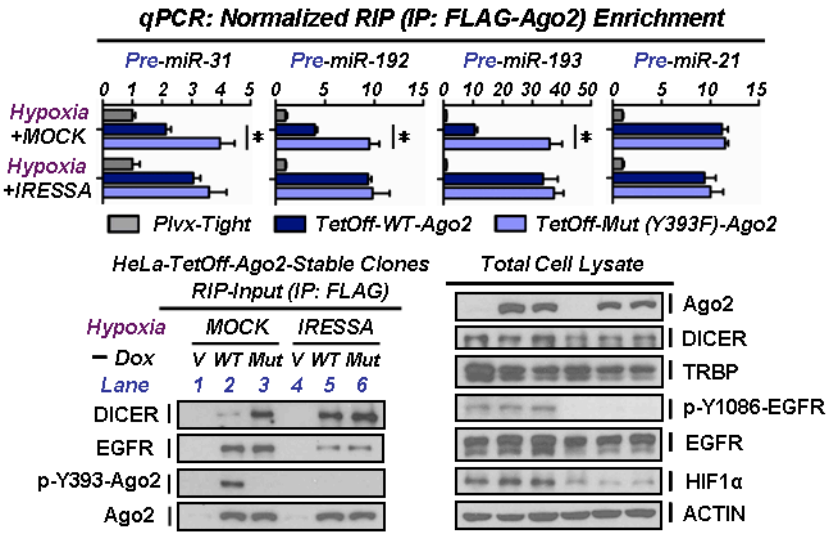

Supplementary Figure 30. The precursors of long-loop mHESM as shown in pre-miR-31, pre-miR-192 and pre-miR-193 but not pre-miR-21 (non-mHESM) were less loaded onto p-Y393-Ago2 under hypoxia. Top, qRT-PCR showing the loading difference between WT and Y393F mutant Ago2 in long-loop mHESM precursors was significantly diminished by TKi (Iressa) treatment under hypoxia. RNA was extracted from anti-FLAG immunoprecipitates in HeLa TetOff-inducible Ago2 stable clones that cultured under hypoxia treated with Mock (DMSO) or Iressa (1 μM) for 24 hr as indicated. Data were normalized to each corresponding negative control (anti-FLAG immunoprecipitate from HeLa TetOff Plvx-Tight (vector control) stable transfectant cultured under hypoxia). Statistical analysis was carried out using Student's *t* test and data are shown as mean ± s.d., *n*=3, * indicates P<0.05. Bottom, IP-western control for RIP (RNA-binding protein immunoprecipitation) assay. p-Y1086-EGFR was used as an indicator for the inhibitory efficacy of Iressa treatment. HIF1α was used as a positive control for cell hypoxic response. β-actin was used as protein loading control.

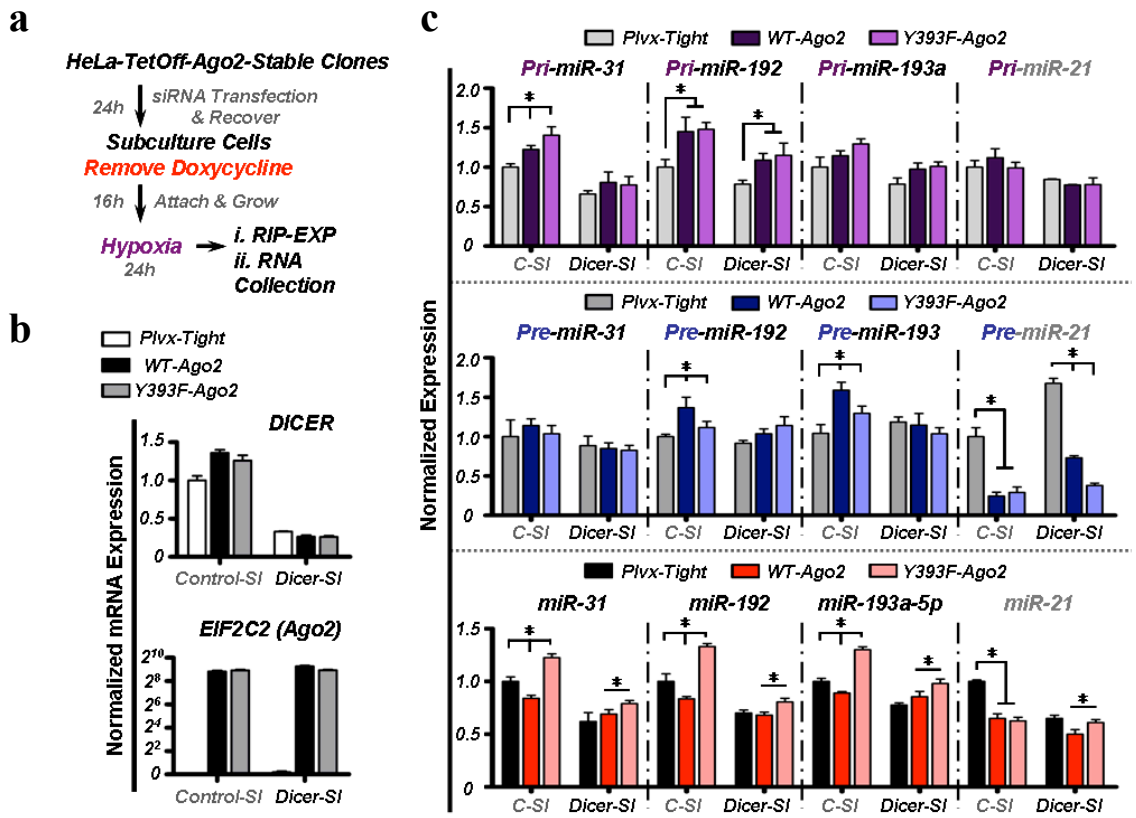

Supplementary Figure 31. The maturation of long-loop mHESM was suppressed by Ago2-Y393 phosphorylation through Dicer. a, Experimental flow chat. **b,** qPCR verification for the mRNA expression of Dicer and Ago2 in HeLa TetOff-inducible Ago2 stable clones expressing control siRNA pool or Dicer siRNA pool (Dharmacon, On-Target Plus siRNA) that were cultured under hypoxia for 24h, as indicated in flow chat **a**. β-actin mRNA was used as internal control. **c,** Normalized expression of mature miR-31, miR-192, miR-193a-5p (long-loop mHESM) and miR-21 (non-mHESM) as well as their precursors and primary transcripts in HeLa TetOff-inducible Ago2 stable clones expressing control siRNA pool or Dicer siRNA pool that were cultured under hypoxia for 24h, as indicated in flow chat **a**. Statistical analysis was carried out using student's *t* test (comparing vector control or WT to Y393F Ago2). Data are shown as mean ± s.d., *n*=3, *indicates P<0.05.

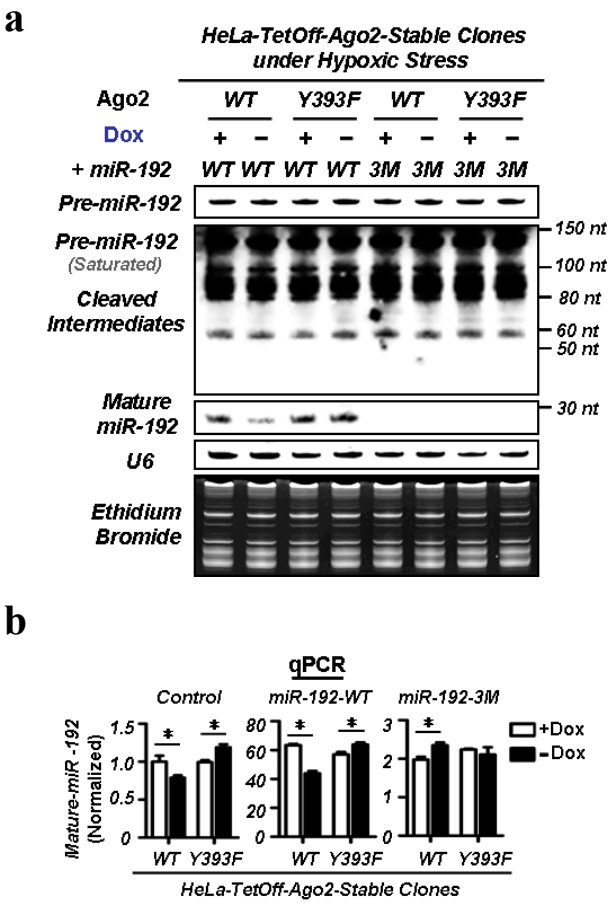

Supplementary Figure 32. The long-loop structure in pre-miR-192 (long-loop mHESM) is required for p-Y393-Ago2-suppressed maturation under hypoxia. a, Pre-miR-192-WT (long-loop) and pre-miR-192-3M (3 nucleotides were mutated, short-loop) were stably expressed in HeLa TetOff-inducible Ago2 stable clones. Total RNA was extracted from the stable transfectants as indicated and subjected to Northern Blot analysis. The detected mature miR-192 signal was too weak compared with the precursors; therefore, data was shown in different exposure time. **b,** Corresponding qPCR analysis. Control, stable expression of vector control; miR-192-WT, stable expression of pre-miR-192-WT; miR-192-3M, stable expression of pre-miR-192-3M in HeLa TetOff-inducible Ago2 stable clones. All the data were first normalized based on U6 internal control and then to the control group (HeLa TetOff WT Ago2, expressing vector control with doxycycline treatment). Statistical analysis was carried out using Student's t test and data are shown as mean ± s.d., *n*=3, * indicates P<0.05.

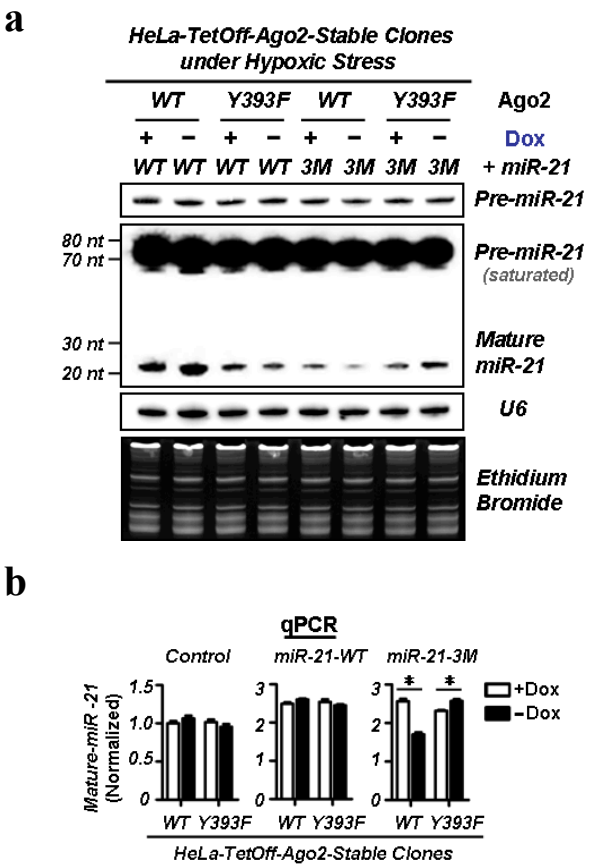

Supplementary Figure 33. Regeneration of a long-loop structure in pre-miR-21-3M renders it to be suppressed by Ago2-Y393 phosphorylation under hypoxia. a, Pre-miR-21-WT (short-loop) and pre-miR-21-3M (3 nucleotides were mutated, long-loop) were stably expressed in HeLa TetOff-inducible Ago2 stable clones. Total RNA was extracted from the stable transfectants as indicated and subjected to Northern Blot analysis. EB staining shows the integrity of RNA samples and U6 was used as RNA loading control. **b,** Corresponding qPCR analysis. Control, stable expression of vector control; miR-21-WT, stable expression of pre-miR-21-WT; miR-21-3M, stable expression of pre-miR-21-3M in HeLa TetOff-inducible Ago2 stable clones. All the data were first normalized based on U6 internal control and then to the control group (HeLa TetOff WT Ago2, expressing vector control with doxycycline treatment). Statistical analysis was carried out using Student's t test and data are shown as mean ± s.d., n=3, * indicates $P<0.05$.

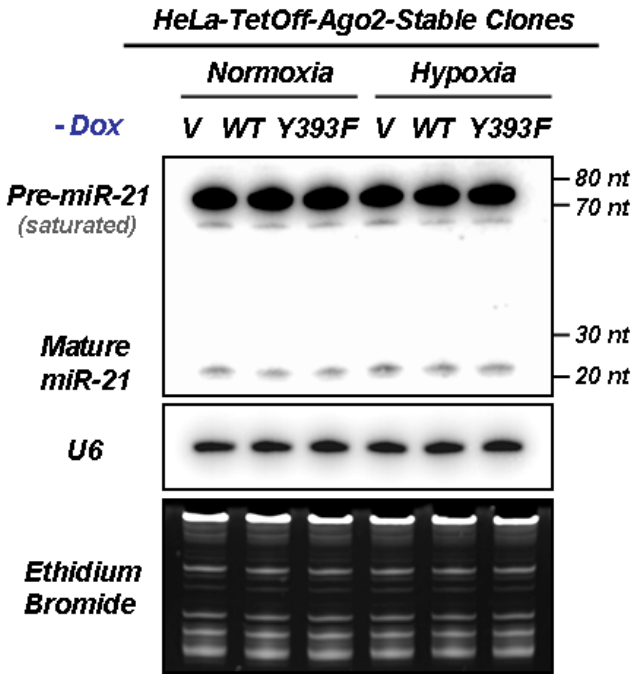

Supplementary Figure 34. The maturation of endogenous miR-21 was not significantly affected by Ago2-Y393 phosphorylation. Total RNA was extracted from HeLa TetOff-inducible Ago2 stable clones cultured under normoxia or hypoxia for 24 hr and subjected to Northern Blot analysis. V, vector control (Plvx-Tight); WT, WT Ago2; Y393F, Y393F Ago2. EB staining shows the integrity of RNA samples and U6 was used as RNA loading control.

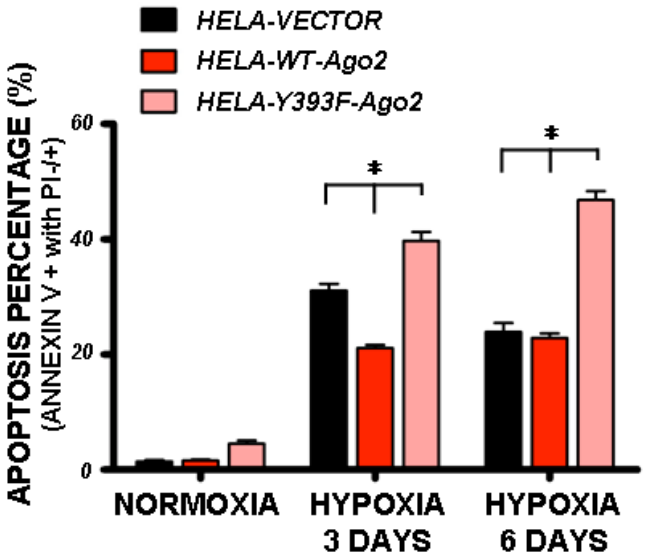

Supplementary Figure 35. Y393F mutant Ago2 cells are more susceptible to apoptosis in response to hypoxia. Apoptosis analysis of HeLa CMV Ago2 stable clones by FACS analysis. Data are shown as mean ± s.d., *n*=3. * indicates P<0.05.

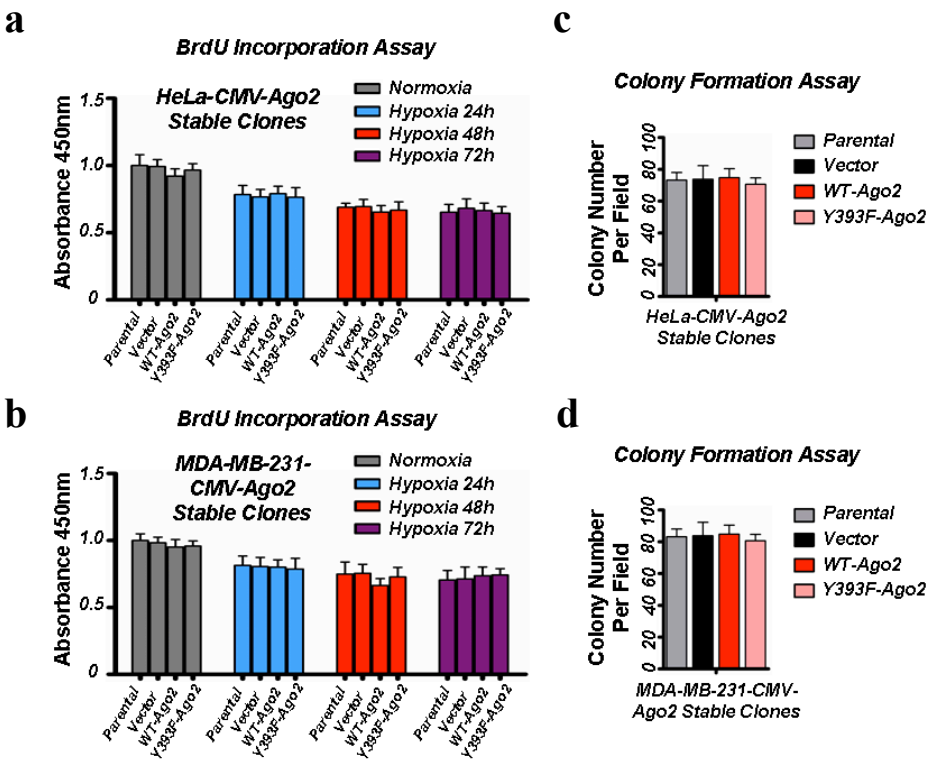

Supplementary Figure 36. Cell proliferation and anchorage-independent cell growth are not significantly affected by WT or Y393F mutant Ago2. Cell proliferation was detected by BrdU Cell Proliferation Assay Kit (Cell Signaling). **a,** 5×10^3 HeLa CMV Ago2 stable transfectant cells, **b,** 2×10^3 MDA-MB-231 CMV Ago2 stable transfectant cells, were seeded at 96 well-plates and cultured under normoxia for 24 hr or hypoxia for 24, 48 and 72 hr. 10 μM BrdU was added to the plate and cells were incubated for 4 hr. Data are shown as mean ± s.d., *n*=5. Soft agar colony formation 15 days after culture. **c,** 1×10^4 HeLa CMV Ago2 stable transfectant cells or **d,** 5×10^3 MDA-MB-231 CMV Ago2 stable transfectant cells on agarose gel. Colonies that grew beyond 50 μm in diameter were scored as positive. Colony number was counted based on three random chosen areas per dish in triplicate. Data are shown as mean ± s.d., *n*=3.

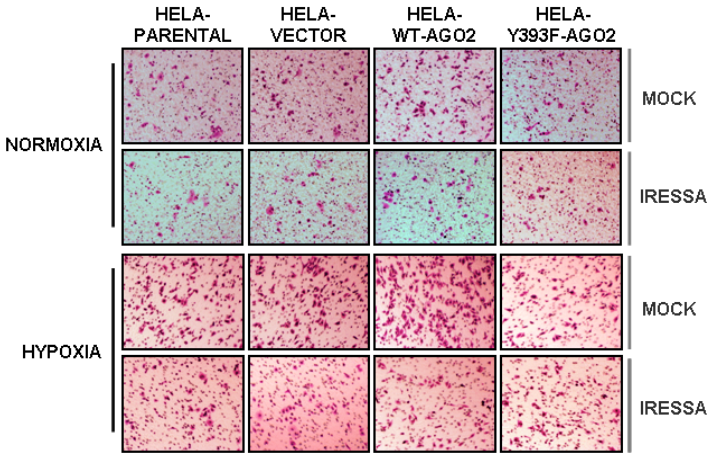

Supplementary Figure 37. Ago2-Y393 phosphorylation enhances cell migration under hypoxia, which can be blocked by Iressa treatment. Representative photographs of *in vitro* cell migration assay shown in Figure 4b. The average number of migrated cells per field (counted visually under a light microscope at original magnification ×200) shown in Figure 4b was calculated based on five randomly selected fields per membrane in triplicate.

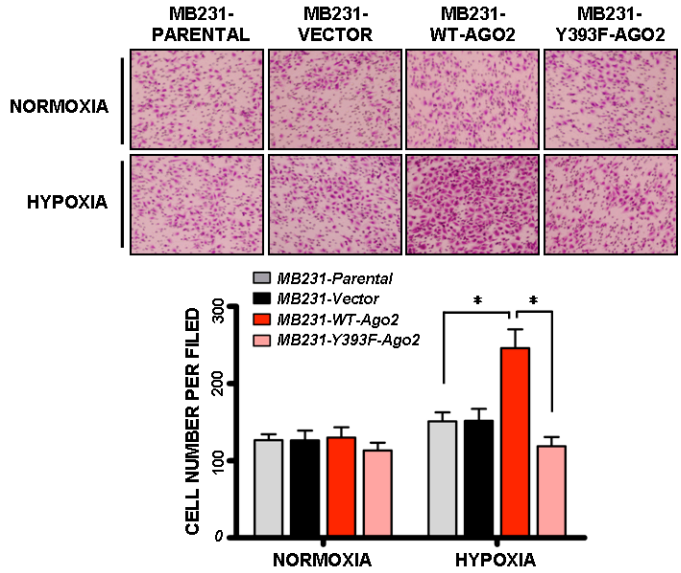

Supplementary Figure 38. Ago2-Y393 phosphorylation enhances cell migration in response to hypoxia. Top, Representative photographs of *in vitro* cell migration assay using MDA-MB-231 CMV Ago2 stable clones cultured under normoxia or hypoxia, as indicated.. Bottom, corresponding quantitation data are shown as mean ± s.d., *n*=3. *indicates P<0.05. The average number of migrated cells per field (counted visually under a light microscope at original magnification ×200) was calculated based on five randomly selected fields per membrane in triplicate.

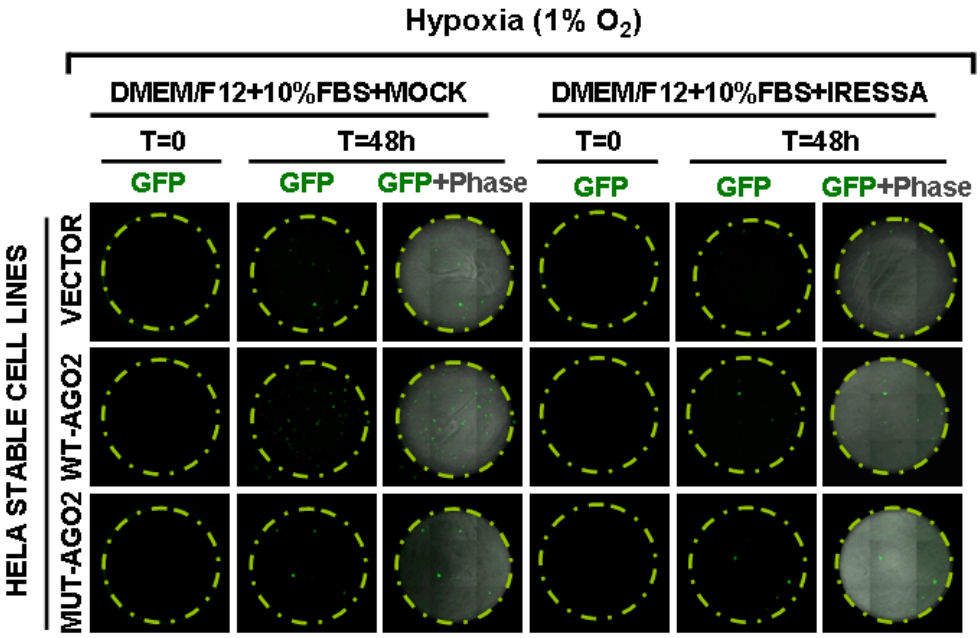

Supplementary Figure 39. Ago2-Y393 phosphorylation mediates EGFR-enhanced cell invasiveness under hypoxia. Representative images of *in vitro* 3-D invasion assay shown in Figure 4c. 9 images were taken by microscope and merged together to show the whole area (marked by yellow circle) for cell invasion in each well (each experimental group contained 5 wells as repeats). HeLa-CMV-Ago2-EF1-CopGFP stable cells are highlighted by their own GFP fluorescence. The number of invaded cells was calculated based on the total cell number in each invasion area as marked by yellow circle after 48 hr as indicated.

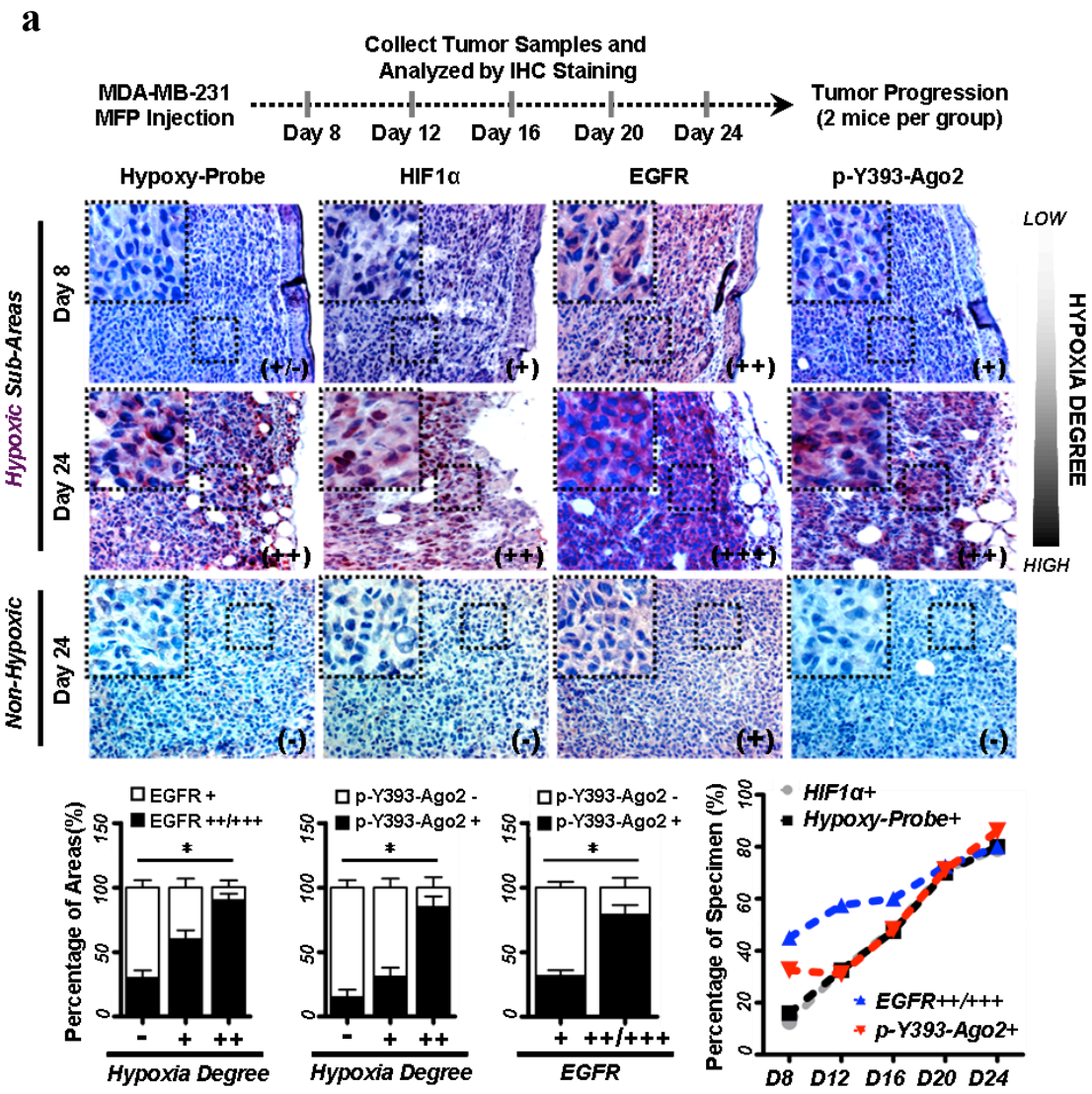
a
Collect Tumor Samples and
Analyzed by IHC Staining
MDA-MB-231
MFP Injection
Day 8
Day 12
Day 16
Day 20
Day 24
Tumor Progression
(2 mice per group)
Hypoxy-Probe
HIF1α
EGFR
p-Y393-Ago2
Hypoxic Sub-Areas
Day 8
Day 24
Non-Hypoxic
Day 24
(+/-)
(+)
(++)
(+)
(++)
(++)
(+++)
(++)
(-)
(-)
(+)
(-)
LOW
HYPOXIA DEGREE
HIGH
EGFR +
EGFR ++/+++
p-Y393-Ago2 -
p-Y393-Ago2 +
Percentage of Areas(%)
Hypoxia Degree
Hypoxia Degree
EGFR
HIF1α+
Hypoxy-Probe+
EGFR++/+++
p-Y393-Ago2+
Percentage of Specimen (%)
D8
D12
D16
D20
D24

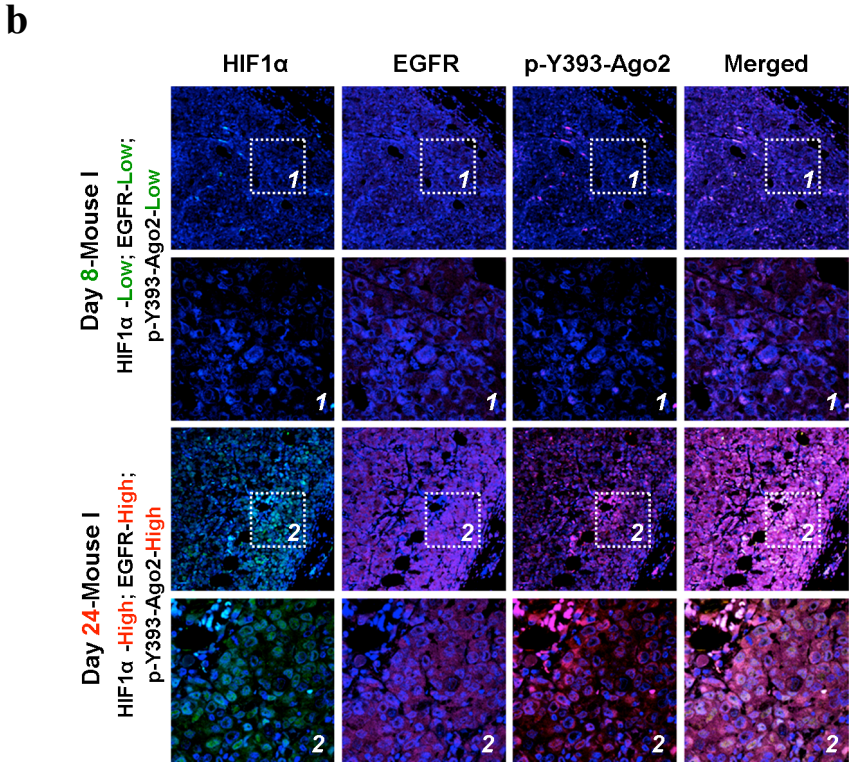

Supplementary Figure 40. The expression of phospho-Y393-Ago2 is upregulated during tumor progression and specifically enriched in the hypoxic tumor subareas. a, Top, experimental design for orthotopic breast cancer mouse model using MDA-MB-231 cells (1×10^6 cells per mouse). Middle, representative IHC images of consecutive sections from collected primary tumors (day 8 and day 24). Bottom, quantitative diagrams showing the expression patterns of EGFR, p-Y393-Ago2 and the degree of hypoxia (based on the average score for hypoxy-probe[42] and HIF1α) in primary tumors. Data at bottom right are shown as mean, n=2. Data at bottom left are shown as mean ± s.d. Statistical analyses were performed by ANOVA or by Student's t test, n=10 (score was based on tumor sub-areas). **b,** Primary tumors (mouse xenograft model) collected on Day 8 and Day 24 were fixed and stained with antibodies against endogenous HIF1α (green), EGFR (magenta), p-Y393-Ago2 (red), and DAPI (blue).

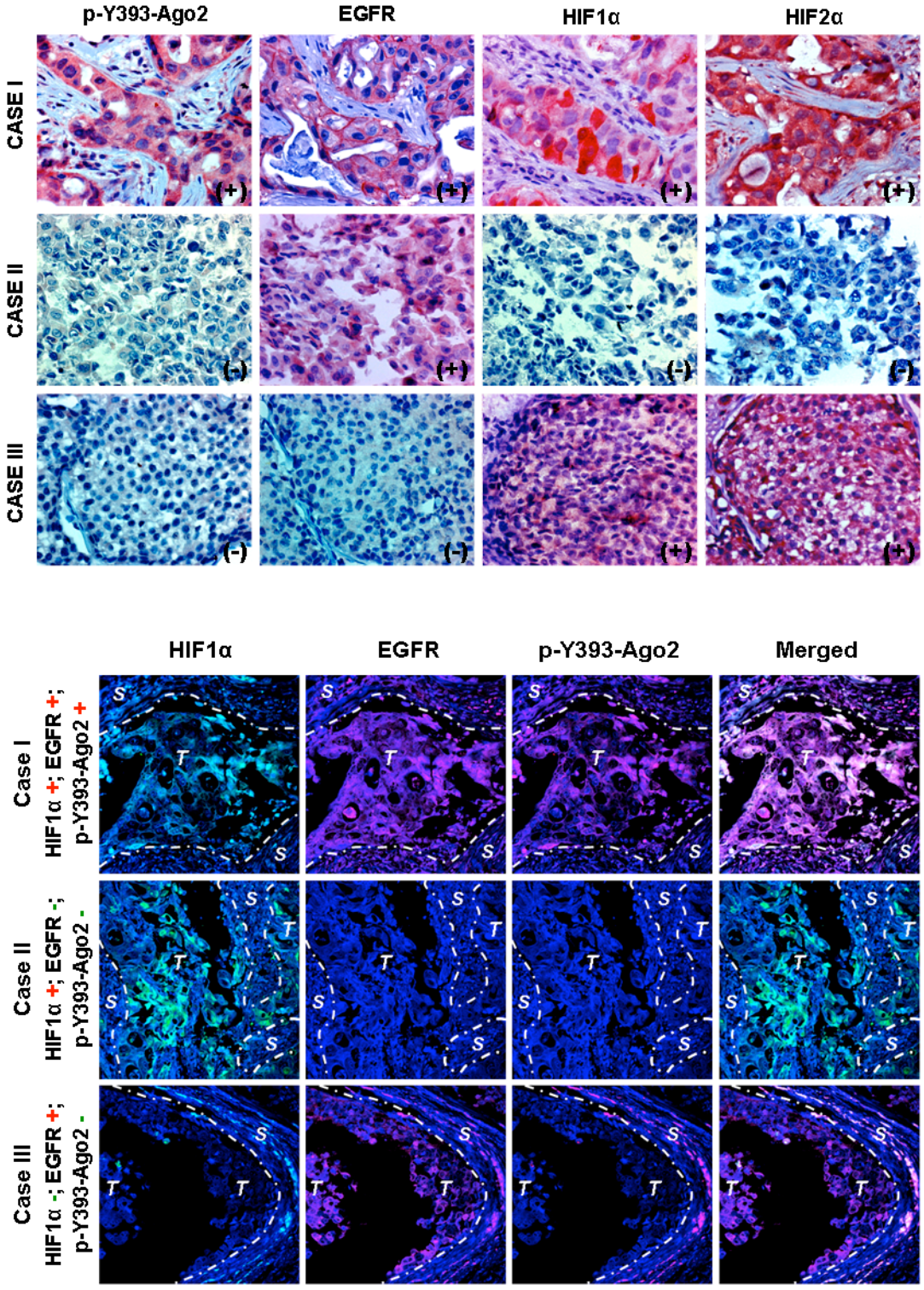

Supplementary Figure 41. phospho-Y393-Ago2 is specifically enriched in human primary breast tumor hypoxic subareas with positive expression of EGFR. a, Human primary breast tumors (128 cases) were examined by IHC staining and the positive correlations between phospho-Y393-Ago2, EGFR and HIF1/2α are shown in Supplementary

Table 1. Representative IHC staining images show that the expression of p-Y393-Ago2 was elevated in hypoxic breast tumor (HIF1/2α positive) with positive expression of EGFR. p-Y393-Ago2 was hardly detected when HIF1/2α or EGFR was not expressed. **b,** Three cases as indicated were chosen to show the colocalization between p-Y393-Ago2, EGFR and the hypoxic microenvironment (indicated by HIF1α) by immunofluorescence analysis. Breast tumor samples were fixed and stained with antibodies against endogenous HIF1α (green), EGFR (magenta), p-Y393-Ago2 (red), and DAPI (blue). S: surrounding tissue; T: human breast tumor area.

Supplementary Table 1.

p-Y393-Ago2 positively correlates with EGFR, HIF1α, HIF2α in human breast carcinoma

	EGFR			*HIF1α*			*HIF2α*		
p-Y393-Ago2	**-/+**	**++**	**+++**	**-/+**	**++**	**+++**	**-/+**	**++**	**+++**
-/+	18(14.1%)	4(3.1%)	3(2.3%)	14(10.9%)	3(2.3%)	9(7.0%)	15(11.7%)	6(4.7%)	5(3.9%)
++	27(21.1%)	7(5.5%)	8(6.3%)	9(7.0%)	8(6.3%)	19(14.8%)	11(8.6%)	12(9.4%)	14(10.9%)
+++	29(22.7%)	9(7.0%)	23(18%)	13(10.2%)	9(7.0%)	44(34.4%)	11(8.6%)	17(13.3%)	37(28.9%)
Total	74(57.8%)	20(15.6%)	34(26.6%)	36(28.1%)	20(15.6%)	72(56.3%)	37(28.9%)	35(27.3%)	56(43.8%)
p-Value	***P<0.04***			***P<0.01***			***P<0.001***		

Expression patterns of p-Y393-Ago2, EGFR, HIF1α and HIF2α in the consecutive sections from human breast tumors were determined and summarized. (-/+): negative-low; (++): positive-medium; (+++): positive-high. The correlation between p-Y393-Ago2, EGFR, HIF1α and HIF2α was analyzed using SPSS 16.0 *Pearson Chi-Square Test*. *P-value* that less than 0.05 was set as the criterion for statistical significance.

Supplementary Methods

Cell Culture and Treatment. Human lung cancer cell line (A-549), human hepatoma cell line (Hep3B), human embryonic kidney cell line (293T), human cervical cancer cell line (HeLa), human mammary epithelial cell lines (MCF-10A and MCF-12A), and human breast cancer cell line (BT-549) were obtained from ATCC. Breast cancer cell line (MDA-MB-231) was gift from Dr. Patricia S. Steeg (National Cancer Institute). RCC4 cell line was kindly given by Dr. Thai Huu Ho from MD Anderson Cancer Center. MCF-10A and MCF-12A cells were grown[43] in DMEM-F12 medium supplemented with 5% horse serum, epidermal growth factor (EGF, 20 ng/ml), insulin (10 μg/ml), cholera toxin (100 ng/ml) and hydrocortisone (0.5 μg/ml). Other cells were grown in DMEM-F12 medium supplemented with 10% fetal bovine serum (FBS). HeLa TetOff-inducible advanced cell line were purchased from Clontech and maintained in DMEM-F12 medium supplemented with 10% Tet-System Approved FBS (Clontech) with both G418 (500 μg/ml) and doxycycline (100 ng/ml). For HeLa TetOff-inducible EGFR and Ago2 stable clones (Plvx-Tight-Vector Control; WT and KD EGFR; WT and Y393F Ago2), cells were maintained in DMEM-F12 medium supplemented with 10% Tet-System Approved FBS (Clontech) with G418 (500 μg/ml), Puromycin (1 μg/ml) and doxycycline (500 ng/ml). The expression of GOI (EGFR or Ago2) was induced after doxycycline removal in accordance with manufacturer's instructions. For hypoxia treatment, cells were seeded at same density in DMEM-F12 medium supplemented with 10% FBS and allowed 4 to 6 hours for adherence in regular cell culture incubator before moving into the hypoxia chamber (INVIV O_2 400, setting as 1% O_2 and 5% CO_2, RUSKINN). HeLa TetOff-inducible stable clones after doxycycline removal were seeded at same density and cultured in regular cell incubator for O/N before moving into the hypoxia chamber. All cell samples were lysed inside of the hypoxia chamber for both IP-WB and RNA extraction. For induction of oxidative stress, cells cultured in DMEM-F12 supplemented with 10% FBS were treated with 500 μM H_2O_2 (Sigma) or 500 μM sodium arsenite (Sigma) for indicated time before collection. Epidermal growth factor (EGF) and Transforming Growth Factor-α (human TGF-α, Sigma) were prepared according to the manufacturers' instructions. Cells were serum-starved and then treated with EGF (20 ng/ml) or TGF-α (10 ng/ml) for indicated time before collection. To induce DNA damage, cells cultured in normal medium were treated with Cisplatin (50 μM) or Etoposide (50 μM) for indicated time before collection. 50 nM AG1478 (Calbiochem) and 1 μM Iressa (Gefitinib) were used to inhibit EGFR kinase activity. 1 μM FM19G11 (Sigma) and 6 μM CAY10585 (Cayman Chemicals) were used to inhibit the transcriptional activity of HIF1/2α.

Antibodies and Peptides. For WB: Flag epitope tag M2 (1: 2,000, Sigma); Flag tag antibody #2368 (1:1,000, Cell Signaling); Anti-HA, 12CA5, (1:2000, Roche Molecular Biochemicals); c-myc antibody 9E10 (1:2,000, Roche Molecular Biochemicals); HIF1α, clone54 (1:500, BD Biosciences); HIF2α, D9E3 #7096 (1:500, Cell Signaling); VHL, PA5-17477, (1:500, Thermo Scientific Pierce Antibodies); antibody against phosphotyrosine, 4G10 (1:3,000, Millipore); Dcp1a, ab47811 (1:1,000, Abcam); Ago2/EIF2C2, ab32381 (1:1,000, Abcam); Argonaute2, C34C6 (1:1,000, Cell Signaling); Anti-AGO2, 11A9 (1:1,000, Sigma); Dicer, H-212 (1:200, Santa Cruz Biotechnology); Dicer, #3363 (1:500, Cell Signaling);

Anti-LAMP1, CD107a (1:1,000, Millipore); GW182, A302-329A (1:1,000, Bethyl Laboratories); Alix, 3A9 (1:1,000, Cell Signaling); TRBP, 46D1 (1:1,1000, Abnova); EEA1, clone14 (1:1,000, BD Biosciences); Hrs, ab56468 (1:1,1000, Abcam); EGFR, sc-03 (1:1,1000, Santa Cruz Biotechnology); LOX, NB100-2527 (1: 1000, Novus Biologicals); p-Y1086-EGFR, #2220, (1:1,000, Cell Signaling); Grb2, 610112, (1:1000, BD Biosciences); p-Y393-AGO2 (1:1,500, homemade); α-tubulin (1:5,000, Sigma); β-actin, AC-74 (1:2,000, Sigma); LaminB1, 4B10, (1:500, Novus Biologicals). For IP: Flag epitope tag M2 (Sigma); EGFR, ab-13 (Thermo Scientific). For IF: GW182, 4B6 (1:50, Abcam); Anti-AGO2, 11A9 (1:200, Sigma); Dcp1a, ab47811 (1:200, Abcam); EGFR, sc-03 (1:150, Santa Cruz Biotechnology); EGFR, ab-13 (1:250, Thermo Scientific); EGFR, ICR10 (1:50, Abcam); Anti-HIF1α, clone EP1215Y (1:200, Millipore); p-Y393-AGO2 (1:2,000, homemade). For IHC: Anti-HIF1α, clone EP1215Y (1:400, Millipore); Anti-HIF2α, NB100-122, (1:300, Novus Biologicals); EGF Receptor, D38B1, (1:100, Cell Signaling); p-Y393-AGO2 (1:3,200, homemade). The following peptides were chemically synthesized for antibody production in mice (Lifetein Conc.), Elisa verification (Lifetein Conc.) and peptide competition assay in immunohistochemistry (IHC). Phospho-Y393-Ago2-peptide: NTDP-pY-VREFG; Non-phospho-Y393-Ago2-peptide: NTDP-Y-VREFG. Random chosen phospho-tyrosine peptides (EGFR-pY1068-Peptide and STAT3-pY705-Peptide) were purchased from Cell Signaling for peptide competition assay in IHC.

Constructs and shRNAs. pcDNA6.A-EGFR, expressing full-length human EGFR with a carboxyl-terminal myc-6×His tag, was constructed and described previously[44]. EGFR extracellular domain plus transmembrane region (EC, amino acids 1-644), EGFR intracellular domain (IC, amino acids 645-1186), EGFR deletion of C-terminal (ΔCD, amino acids 1-955) were subcloned into pcDNA6.A/myc-His vector (Invitrogen). Kinase-dead EGFR^{K721R} (KD EGFR) was generated using the Quick-Change Site-Directed Mutagenesis Kit according to the manufacturer's instruction (Stratagene). Full-length human Ago2 was amplified from the cDNA of HeLa cells and subcloned into a modified pCMV5 vector containing an N-terminal FLAG tag. Functional domains of Ago2 (FDM1: 1-372 aa; FDM2: 1-517 aa; FDM3: 227-860 aa; FDM4: 373-860 aa; FDM5: 518-860 aa) were subcloned into the same pCMV5 vector for mapping protein regions binding with EGFR. For *in vitro* pull-down and kinase assays, full-length Ago2, Ago2-FDM2 and Ago2-FDM4 were subcloned into pGEX6P1-GST vector. For generating YFP-interaction system, full-length EGFR and Ago2 were subcloned into pBABE-CMV-DEST-Neo (fused with YFPn) and pBABE-CMV-DEST-Puro (fused with YFPc) respectively. The YFP-interaction system vectors were gifts from Dr. Zhou Songyang at Baylor College of Medicine (Houston, Texas). For generating HeLa TetOff-inducible stable clones, full-length WT EGFR, KD EGFR and WT Ago2 (with fused C-terminal FLAG tag) were subcloned into Plvx-Tight-Puro vector (Clontech). For generating Ago2 stable clones, full-length Ago2 (with fused C-terminal FLAG tag) were subcloned into pCDH-CMV-MCS-EF1-Puro (CD510B-1) and pCDH-CMV-MCS-EF1-copGFP (CD511B-1, System Biosciences) vectors. All mutant constructs of Ago2 (Y393F, Y393D, Y393E) were generated using the Quick-Change Site-Directed mutagenesis kit (Stratagene) and confirmed by DNA sequencing. For live-cell imaging, WT-EGFR fused with C-terminal GFP was constructed and described previously[44]. Full-length human Ago2 was subcloned into

pTagBFP-C vector (with N-terminal BFP tag). Human pre-microRNA Expression Constructs Lenti-miR-192-WT (MI0000234) and Lenti-miR-21-WT (MI0000077) were purchased from System Biosciences. Lenti-miR-192-3M and Lenti-miR-21-3M were generated using the Quick-Change Site-Directed mutagenesis kit (Stratagene) and confirmed by DNA sequencing. The pre-miRNA sequence of miR-192-3M is: GCCGAGACCGAGUGCACAGGGCUCUGACCUAUGAAUUGACAGCCAGUGGUGUG GUCUCCCCUCUGGCUGCCAAUUCCAUAGGUCACAGGUAUGUUCGCCUCAAUGC CAGC; the pre-miRNA sequence of miR-21-3M is: UGUCGGGUAGCUUAUCAGACUGAUGUUGACUUAUUAAUCUCAUGGCAACACC AGUCGAUGGGCUGUCUGACA (red color highlights the nucleotides that were mutated). RNA interference was performed using lentiviral short hairpin RNAs (shRNAs) from MISSION^{TM} TRC-Hs (human) shRNA Library according to the instructed protocol. Lentiviral packaging system, pCMV-dR8.2 dvpr (#8455) and pCMV-VSVG (#8454), pBabe-puro-WT-VHL (#19234) were bought from Addgene. The oligo sequences of shRNAs are listed below and confirmed by DNA sequencing. ON-TARGETplus Non-Targeting Pool (D-001810-10) and ON-TARGETplus DICER1 siRNA SMARTpool (targeting CDS of Dicer) were purchased from Dharmacon, Thermo Scientific.

Scrambled Control (#1864, Addgene):
CCTAAGGTTAAGTCGCCCTCGCTCGAGCGAGGGCGACTTAACCTTAGG;

EGFR shRNA-E1 (TRCN0000121067):
CCGGGCTGCTCTGAAATCTCCTTTACTCGAGTAAAGGAGATTTCAGAGCAGCTTT TTG (targeting 3' UTR of EGFR);

EGFR shRNA-E2 (TRCN0000121068):
CCGGGCCACAAAGCAGTGAATTTATCTCGAGATAAATTCACTGCTTTGTGGCTTT TTG (targeting CDS of EGFR);

Grb2 shRNA-1 (TRCN0000029372):
CCGGGATCTACATCTGTCTCCAGAACTCGAGTTCTGGAGACAGATGTAGATCTTT TT (targeting CDS of Grb2);

Grb2 shRNA-2 (TRCN0000029373):
CCGGCAGATATTCCTGCGGGACATACTCGAGTATGTCCCGCAGGAATATCTGTTT TT (targeting CDS of Grb2);

HIF1α shRNA#1 (TRCN0000003810):
CCGGGTGATGAAAGAATTACCGAATCTCGAGATTCGGTAATTCTTTCATCACTTT TT (targeting CDS of HIF1α);

HIF1α shRNA#2 (TRCN0000010819):
CCGGTGCTCTTTGTGGTTGGATCTACTCGAGTAGATCCAACCACAAAGAGCATTT TT (targeting 3' UTR of HIF1α);

EPAS1/HIF2α shRNA#1 (TRCN0000003806):
CCGGCAGTACCCAGACGGATTTCAACTCGAGTTGAAATCCGTCTGGGTACTGTTT
TT (targeting CDS of HIF2α);

EPAS1/HIF2α shRNA#2 (TRCN0000003805):
CCGGGCGCAAATGTACCCAATGATACTCGAGTATCATTGGGTACATTTGCGCTTT
TT (targeting CDS of HIF2α).

Mass spectrometry. Mass spectrometric analysis was performed as previously described[45]. Briefly, endogenous EGFR was purified by immunoprecipitation with anti-EGFR antibody (Ab-13) and analyzed by SDS-PAGE. All the protein bands co-immunoprecipitated with EGFR was excised and analyzed by nanoelectrospray mass spectrometry for protein ID identification. To identify phosphorylation sites of Ago2, we purified FLAG-tagged Ago2 that co-expressed with EGFR in 293T cells and analyzed the results by SDS-PAGE and Western-Blot. The protein band corresponding to Ago2 was excised and subjected to in-gel digestion with trypsin. After being isolated from the gel, samples were analyzed by nanoelectrospray mass spectrometry, using an Ultimate capillary LC system (LC Packings) coupled to a QSTARXL quadrupole time-of-flight mass spectrometer (Applied Biosystem/MDS Sciex). All the identified phospho-residues were further confirmed by manual interpretation of the spectra.

RNA Deep Sequencing and Hierarchical Clustering Analysis. Customized Next-Generation RNA deep sequencing, including both small RNA application and whole transcriptome analysis, was performed according to the standard procedure instructed by Applied Biosystems. All the RNA sequencing data were deposited to GEO with accession number GSE44804. Briefly, total RNA was extracted from HeLa stable clones expressing scrambled control (S) or EGFR shRNA-E1 (E1) that were seeded at same density and cultured under normoxia or hypoxia (1% Oxygen) for 24 hours. All RNA samples passed quality test with RIN-values greater than 8 as measured by Agilent Technologies Bioanalyzer, were subjected to RNA deep sequencing. *For whole transcriptome analysis*, SOLiD fragment colorspace transcriptome reads (50nt) were mapped to the human genome (hg19) and assigned to ensemble transcripts using Bioscope 1.3.1 (Life Technologies). The values of reads per kilobase per million reads (RPKM) were determined by Bioscope 1.3.1 CountTags tool using default parameters. Primary alignments with a minimum mapping quality of 10 and minimum alignment score of 10 were counted. *For small RNA analysis,* library inserts were size selected between 18 and 40nts and analyzed using CLC Genomics Workbench 4.7.1. 35nt colorspace reads were trimmed of adaptor sequence and mapped against human pre-miR sequences (miRBase version 16.0). Values of reads per million mapped reads (RPM) were based on mapped reads with no more than 2 mismatches total. A read was considered to come from a mature miRNA if it mapped to pre-miRNA sequences with no more than three upstream or downstream bases, and missing no more than two upstream or downstream bases from predicted mature or mature* sequences as defined in miRBase version 16.0. All the other pre-miRNA mapped reads were assigned as pre-miRNA signal. *For Hierarchical*

Clustering Analysis, Data files from small RNA or whole transcriptome analysis were first filtered based on the normalized expression value RPM (cutoff genes with all mapped reads ≤100 counts) or RPKM (filtered with count value ≥0.5 RPKM). Gene expression profiles were then transformed into Log2 data for comparing expression differences. For miRNA maturation analysis, we transformed the original expression data (Log2 transformed) into relative expression of pre- and mature miRNA levels that affected by EGFR knockdown (as calculated by expression change-fold). We define relative expression of pre- or mature miRNA＝Log2 (pre- or mature miRNA in HeLa scrambled control)-Log2 (pre- or mature miRNA in HeLa EGFR shRNA-E1 stable clone). For identifying the mRNAs that regulated by EGFR and likely targeted by top-scoring mHESM, mRNAs modulated by EGFR knockdown (with Log2 fold-change affected by EGFR ≥ 0.4 or ≤ -0.4) were sorted and over-lapped with the predicted mRNAs (based on published data and TargetScan prediction with total context score ≤ -0.20) that targeted by top-scoring mHESM. For all the other analysis, Log-transformed gene expression files were further normalized by mean centering to correct average gene expression from all the samples as log2-ratio of 0. Centroid Linkage Clustering was performed and the interactive graphical results from Cluster were further analyzed by TreeView for displaying heatmaps.

qRT–PCR assays and Northern-Blot analysis. qRT–PCR assays as described previously[26] were performed to measure the expression of mRNA, pri-, pre- and mature miRNAs with some adaptations. Briefly, cells were washed twice with PBS and immediately lysed in QIAzol. For mRNA, pri- and mature miRNA detection, half of the lysed sample was subjected to total RNA extraction using miRNeasy Mini Kit (Qiagen). For pre-miRNA detection, the other half of the lysed sample was subjected to small RNA fraction purification using the miRvana miRNA isolation kit (Ambion). To measure the expression of mRNA or pri- or pre-miRNAs, cDNA was synthesized from 1ug purified total RNA or 500ng purified small RNA (size-fractioned) by SuperScript III First-Strand cDNA synthesis system using random hexamers (Invitrogen) according to the manufacturer's instructions. qPCR was performed using real-time PCR machine (iQ5, BioRad). For detection of mature miRNAs, TaqMan MicroRNA assay kit (Applied Biosystems) was used in accordance with the manufacturer's protocol. qPCR was performed using 7500 Fast Real-Time PCR System (Applied Biosystems). All the data analysis was performed using the comparative Ct method. Results were first normalized to internal control β-actin mRNA or U6 snRNA, which were almost not affected by hypoxia or EGFR knockdown, and then the relative expression of pri-, pre- or mature miRNAs in response to hypoxia was given by normalized expression level under hypoxia relative to the corresponding normalized expression under normoxia. Each RNA sample (except for RIP experiment) was analyzed in duplicate and presented as an average of two independent RNA preparations. The sequences of qPCR primers are given in the Supplementary Information. Northern-Blot analysis was performed as described previously[46]. miRCURY LNA probes (targeting hsa-miR-21 or hsa-miR-192, Exiqon) and DNA oligonucleotide (5′- GGGGCCATGCTAATCTTCTCTGTATCGTTCCAATTTTAGT ATATGTG-3′; Sigma) targeting U6 (internal control) were end-labeled with [γ-32P] ATP and used as probes for Northern Blot analysis.

Immunoprecipitation and immunoblotting. Immunoprecipitation and immunoblotting were performed as previously described[45]. Briefly, cells were washed twice with cold PBS and scraped into lysis buffer containing complete protease inhibitors (all the above steps were done inside of the hypoxia chamber). After brief sonication, cell lysates were centrifuged at 14,000*g* for 20 min at 4°C to remove insoluble cell debris and then subjected to IP-WB.

Iodixanol continous density gradient. Optiprep iodixanol density media was obtained from Sigma-Aldrich. Continuous density gradients were performed as described previously with some adaptations[31]. Briefly, HeLa cells seeded at the same density were either cultured under normoxia or hypoxia (1% Oxygen) for 24 hr before collection. Cells were then washed twice in PBS and re-suspended with PBS. 10% of the suspended cells were lysed by RIPA buffer as the whole cell lysate input for later on protein analysis. The rest of the cells were re-suspended in 500 µl 0.25 M sucrose, 4 mM $MgCl_2$, 8.4 mM $CaCl_2$, 10 mM EGTA, 50 mM Hepes-NaOH at pH 7.0 with complete protease inhibitors. Cells were lysed by 40 strokes of dounce homogenizer and 10 passages through a 26-gauge needle, and centrifuged at 1,000*g* for 5 min twice to remove cellular debris and nuclei. Continuous 0–30% optiprep gradients were prepared in 78 mM KCl, 4 mM $MgCl_2$, 8.4 mM $CaCl_2$, 10 mM EGTA and 50 mM Hepes-NaOH at pH 7.0 using a gradient mixer (gradient station, Biocomp Instruments). Postnuclear supernatant was added to the top of 13 ml gradients and centrifuged at 90,000*g* for 20 h. Fractions (0.5 ml per fraction) were collected from the bottom of the gradient using a fraction collector (BioFrac, BioRad) that measures conductivity to verify continuity of gradients. For analysis, 30 µl whole cell lysate input (with total volume 500 µl) was loaded along with 30 µl protein samples from each fraction (500 µl per fraction) in SDS-PAGE, and subjected for WB and quantified by Odyssey Infrared Imaging System.

Generation of stable clones expressing GOI and shRNAs. YFP-interaction system (in HTC-1080 and HeLa cells) and RCC4 stable transfectants expressing vector control or WT-VHL were generated by retroviral infection. All the other stable clones expressing GOI or shRNAs were generated by Lentiviral infection. For retroviral infection, packaging plasmids (gag/pol and VSV-G) were co-transfected with pBABE-Neo-EGFR-YFPn or pBABE-Puro-Ago2-YFPc into 293T cells, and viral particles were harvested at 48 hr post-transfection. HTC-1080 and HeLa cells were infected with one or co-infected with both viruses for 24 hr in the presence of polybrene (10 µg/ml) and subsequently selected by G418 (1,000 µg/ml) or puromycin (1 µg/ml) or G418 (500 µg/ml) together with puromycin (0.5 µg/ml). For RCC4 stable transfectants, pBabe-puro-vector or pBabe-puro-HA-WT-VHL together with pCL-Ampho (optional) was transfected into phoenix cells, and viral particles were harvested at 48 hr post-transfection. The other steps were the same as described above. HeLa TetOff-inducible stable clones were generated following the protocol instructed by Clontech. Briefly, 293T cells were seeded in DMEM-F12 medium supplemented with 10% Tet-System Approved FBS (Clontech) for 24 hr before transfection. Lentiviral packaging plasmids (generation II), pCMV-dR8.2-dvpr and pCMV-VSVG, were co-transfected with lentiviral constructs expressing GOI (plvx-tight-vector; WT or KD EGFR; WT or Y393F Ago2) into Tet-Free 293T cells. Viral particles were harvested at 48 hr post-transfection and further infected into Tet-Free targeting cells (HeLa TetOff Advanced Cell Line) for 24 hr in

the presence of polybrene (10 μg/ml). At 48 hr post-infection, cells were selected by both G418 (500 μg/ml) and puromycin (1 μg/ml) in DMEM-F12 medium supplemented with 10% FBS and doxycycline (500 ng/ml) for generating stable clones without induction of GOI. For generating EGFR shRNA, Grb2 shRNA, HIF1α shRNA, HIF2α shRNA and other Ago2 stable clones (including knocking down endogenous EGFR in HeLa CMV Ago2 stable clones and stable expression of miR-192-WT, miR-192-3M, miR-21-WT and miR-21-3M in HeLa TetOff Ago2 stable clones), similar lentiviral infection procedure (with no restriction of Tet-Free) was performed. Stable clones were generated either by puromycin (2 μg/ml in HeLa; 1 μg/ml in MDA-MB-231) selection or sorted twice by flow cytometry based on the expression of GFP.

miRNA-Reporter Assay. Oligonucleotides complementary to the sequences of mature miR-21, miR-31, miR-192, miR-193a-5p or all of the later three seeding sequences were ligated into pMIR-Reporter (Ambion) and verified by DNA sequencing. HeLa TetOff Ago2 stable clones were co-transfected with each miR-Reporter (firefly luciferase) together with internal control (pRL-Renilla luciferase control reporter) and cultured under normoxia or hypoxia for 36-48 hr after doxycycline removal. The luciferase activity of miR-Reporter was determimed by the ratio of firefly to renilla luciferase as measured by the Dual-Luciferase Reporter Assay System (Promega) and further normalized to the one of vector control cultured under normoxia. The oligonucleotide sequences for each pMIR-Reporter are listed in the Supplementary Information.

RNA-Binding Protein Immunoprecipitation (RIP-Assay). RNA-Binding Protein Immunoprecipitation Kit (Magna RIP, Millipore) was used for RIP-Assay, according to the manufacturer's instruction. Briefly, HeLa TetOff Ago2 stable clones were cultured under hypoxia for 24 hr after doxcycline removal and then treated with MOCK (DMSO) or TKI (Iressa, 1 μM) for 8 hr before collection. Cells were lysed in RIP Lysis Buffer with both protease inhibitor and RNase inhibitor, and 5% of the total cell lysates were used for Western-Blot analysis as experimental control. FLAG antibody was bound to the magnetic beads and added into each RIP reaction (RIP lysate in RIP immunoprecipitation buffer with RNase inhibitor) for incubation O/N at 4 °C. Beads were washed 6 times in cold RIP washing buffer and 10% of the beads were kept as RIP-input to show the precipitated protein quantity of WT or Y393F Ago2. Proteins were digested in Protease K buffer at 55 °C for 30 min, and total RNA was extracted using miRNeasy Mini Kit (Qiagen). A 15-μl elution of RNA (with total volume 30 μl) was used for cDNA systhesis and further analyzed by qPCR. Except for first-strand synthesis, the procedure for RIP-Assay using HeLa TetOff Ago2 stable clones expressing ON-TARGET control siRNA pool or ON-TARGET Dicer1 siRNA SMART pool is similar. After RNA purification from anti-FLAG immunoprecipitates, 15-μl elution of RNA (with total volume 30 μl) was synthesized into cDNA using SuperScript III with random hexamers (Invitrogen) for detection of miRNA precursors, while another 15-ul elution of RNA was reversely transcribed into cDNA using TaqMan MicroRNA assay kit for detection of mature miRNAs.

In vitro Pull-Down Assay. Recombinant GST-Ago2 (full-length), GST-Ago2-FDM2,

GST-Ago2-FDM4 and GST were expressed in *E. coli* (BL-21) and purified by glutathione-sepharose beads. Similar quantity of protein samples were incubated with *in vitro* transcription and translation lysates of myc-tagged full-length EGFR (pCDNA6.a-WT-EGFR), produced by TNT coupled reticulocyte lysate system (Promega), in binding buffer (25 mM Tris-HCl, pH 7.5, 125 mM NaCl, 1 mM phenylmethylsulfonyl fluoride, 1 μg of leupeptin/ml, 1 μg of aprotinin/ml, and 1 μg of pepstatin/ml) for O/N at 4 °C. Beads were washed five times with Tris-buffered saline and subjected to SDS-PAGE for autoradiography.

In vitro Kinase Assay. Recombinant GST-WT-Ago2 and GST-Y393F-Ago2 were incubated with or without (negative controls) purified human EGFR (E2645, Sigma) in HTScan 1× tyrosine kinase buffer (Cell Signaling) supplemented with 200 μM cold ATP and 2.5 mM DTT for 40 min at 30 °C. The reaction of purified EGFR without substrate was carried out under the same condition as another negative control. Kinase Assay was stopped by 8.5% phosphoric acid, subjected to SDS-PAGE and analyzed by Western-Blot using 4G10 antibody.

Confocal Microscopy Analysis. Confocal Microscopy analysis was performed as described previously[47]. Briefly, cells after treatment were washed three times with cold PBS, fixed in 4% paraformaldehyde for 20 min at RT. For experiments under hypoxia, cells were washed with cold PBS and then added with 4% paraformaldehyde before moving out of the hypoxia chamber. Cells were then permeabilized with 0.5% Triton X-100 for 10 min, and incubated with 5% bovine serum albumin for 1 hr. After that, cells were incubated with primary antibodies overnight at 4°C, and then washed with PBS, and further incubated with the appropriate secondary antibody diluted at 1:300 and tagged with Alexa 488, Alexa 568 or Alexa 647 (Molecular Probes) for 1 hr at room temperature. Nuclei were stained with 4,6-diamidino-2-phenylindole (DAPI) before mounting. Confocal fluorescence images were captured using a Zeiss LSM710 laser microscope. In all cases, optical sections through the middle planes of the nuclei, as determined using nuclear counterstaining, were obtained. For Live-Cell imaging, HeLa cells were co-transfected with EGFR-GFP and BFP-Ago2, and then cultured under normoxia or hypoxia for 24 hr. 50 nM Lyso-Tracker (Red DND-99, Invitrogen) was added into cells right before confocal analysis. Alternatively, HeLa cells co-expressing EGFR-GFP and BFP-Ago2 was further transduced with CellLight Rab7-RFP (CellLight late endosome-RFP, Invitrogen) according to the manufactory's instruction for 24 hr, and after that, cells were cultured under normoxia or hypoxia for 24 hr before confocal analysis.

Duolink Assay (in situ Proximity Ligation Assay). In situ Proximity Ligation Assay was performed according to manufacturer's instructions (OLINK BIOSCIENCE). Briefly, HeLa stable transfectants expressing scrambled control or shRNAs (targeting Grb2 or HIF1α or HIF2α) were seed on 8-well chamber slides and cultured under normoxia or hypoxia for 24 hr. Cells were then washed (inside of the hypoxia chamber), fixed, permeablized and blocked before primary antibody (against endogenous EGFR and Ago2) incubation at 4°C overnight. After washing, secondary antibodies conjugated with oligonucleotides (Minus and Plus) were

added into each reaction and incubated for 1 hr at 37°C. Cells were washed before adding ligation solution and further incubated at 37°C for 30 min. Finally fluorescently labeled oligonucleotides (FITC in our case) together with Polymerase were added into each reaction for amplification of the original ligated nucleotide circles. The positive signal is visualized as distinct fluorescence spot and each spot represents one cluster of protein-protein interaction.

Cell Apoptosis Analysis. Evaluation of apoptosis by the annexin V-propidium iodide (PI) binding assay was performed according to the standard protocol. APC-Annexin V and propidium iodide (PI) (BD Biosciences) were prepared according to the manufacturer's instructions. The extent of apoptosis was quantified as percentage of annexin V-positive cells.

Cell Proliferation Assay. Cell proliferation was measured by BrdU Cell Proliferation Assay Kit (#6813, Cell Signaling) according to the manufacturer's instructions.

Soft Agar Assay. HeLa Ago2 stable clones (1×10^4cells) and MDA-MB-231 Ago2 stable clones (5×10^3cells) were resuspended in DMEM containing 10% FBS with 0.5% agarose and layered on top of 1.0% agarose in DMEM on 24-well plates. A 500-μl normal culture medium containing 1 μg/ml puromycin was added to the top of each well and changed every five days. Cultures were maintained for 15 days. Colonies that grew beyond 50 μm in diameter were scored as positive. Each experiment was done in triplicate.

Cell Migration Assay. Cell migration assays were performed in Biocoat transwell filter inserts (8um, 24-well plates, BD Biosciences) as described previously with some adaptations. Briefly, Cells were pre-treated with MOCK (DMSO) or TKI (Iressa, 1 μM) for 6 hr before trypsinization. DMEM-F12 containing 10% FBS with MOCK or TKI was added to the bottom chamber. Cell suspensions (2×10^4 HeLa Ago2 stable clones or 1×10^4 MDA-MB-231 Ago2 stable clones) in serum-free DMEM-F12 with MOCK or TKI were added to the upper chamber. After migration for 18 hr under normoxia or hypoxia, cells on the top surface of the membrane were removed and the remaining cells, which migrated through the inserts, were fixed and stained with crystal violet. The average number of migrated cells per field (counted visually under a light microscope at original magnification ×200) was calculated based on five randomly selected fields per membrane in triplicate.

Three-Dimensional Invasion Assay. The 3-D Oris^{TM} cell invasion assay was performed according to the manufacturer's instructions (Platypus Technologies). Briefly, 100ul of the BME coating solution was added into the wells (96-well-black plate, Platypus Technologies) and incubated in a humidified cell culture chamber for 15-30 min for solidification. Oris^{TM} cell seeding stoppers were inserted perpendicular to each well bottom and fully engaged with the bottom of each well. HeLa Ago2 stable clones (5×10^4 cells) were resuspended in 100ul DMEM-F12 medium supplemented with 10% FBS and puromycin (1 μg/ml) with Mock (DMSO) or Iressa (1 μM). Cell suspensions were added into each well through one of the side ports of the Oris^{TM} cell seeding stopper and allowed O/N for complete cell attachment. Stoppers were removed by the Oris^{TM} stopper tool. The top medium of each well was removed and any unattached cells were cleared by gently washing with PBS. 40ul Oris^{TM}

BME stock reagent mixed with Mock or Iressa (1 μM) was added into each well to create a 3-D BME overlay. Then, the plate was incubated in a humidified cell culture chamber for 30 min for polymerization of the 3-D BME overlay. Finally, 100 μl of serum-free cell culture medium with Mock or Iressa (1 μM) was added on the top of the 3-D BME overlay. We recorded full-images of the well center (with no cells at T_0) at different time points (T=0, T_{24}=24 hr and T_{48}=48 hr) using a Zeiss LSM710 laser microscope. Invasion capacity was reported as the average number of cells (5 different wells per experimental group) that invaded into the center of wells in 48 hr.

Orthotopic xenograft breast cancer model. Orthotopic breast cancer mouse model was performed as previously described[47]. Briefly, MDA-MB-231 cells (1×10^6 cells) were injected into the mammary fat pads of nude mice (at Day 0). Two hours before sacrifice, mice were intraperitoneally injected with Hypoxy-probe (pimonidazole hydrochloride, HPI, Inc.) at a dosage of 60 mg/kg body weight according to the manufacturer's instructions. Five series of tumor samples (2 mice per group) were collected every 4 days (started from Day 8 to Day 24) and analyzed by IHC staining. All animal procedures were conducted under the guidelines approved by the Institutional Animal Care and Use Committee (IACUC) at MD Anderson Cancer Center (Protocol Number 06-87-06139).

Immunohistochemical Staining. Immunohistochemical staining was performed as previously described[48]. To validate the specificity of p-Y393-Ago2 antibody in IHC, we performed peptide competition assay by staining human breast tumor sample with p-Y393-Ago2 antibody blocked with Mock or phospho-Y393-Ago2-peptide or non-phospho-Y393-Ago2-peptide, or two randomly chosen phospho-tyrosine peptides, EGFR-pY1068-Peptide and STAT3-pY705-Peptide (Cell Signaling), at the same concentration (1 μg/ml). The procedure for IHC staining in orthotopic xenograft model was similar. The hypoxy-probe was stained using the Hypoxyprobe™-1 Plus Kit (HPI, Inc.). Universal LSAB™+ Kit/HRP (Dako) was used for detection of p-Y393-Ago2 in mouse xenograft tumor samples. Human breast tumor tissues samples were obtained under the guidelines approved by the Institutional Review Board at MD Anderson Cancer Center.

Primer Information for qPCR

Primers for qPCR	**5′ to 3′**	**Notes**
U 6-Forward:	CTCGCTTCGGCAGCACA	Internal Control
U 6-Reverse:	AACGCTTCACGAATTTGCGT	Internal Control
Pre-mir15b-Forward:	AGCACATCATGGTTTACATGC	*
Pre-mir15b-Reverse:	CTAGAGCAGCAAATAATGATTCG	*
Pre-mir16-1-Forward:	GCAGCACGTAAATATTGGCGT	*
Pre-mir16-1-Reverse:	CAGCAGCACAGTTAATACTGGAGA	*
Pre-mir16-2-Forward:	GCACGTAAATATTGGCGTAGT	*
Pre-mir16-2-Reverse:	AAGCAGCACAGTAATATTGGTG	*
Pre-mir24-1,2-Forward:	CTCCCGTGCCTACTGAGCT	*
Pre-mir24-1,2-Reverse:	CCCTGTTCCTGCTGAACTGAG	*
Pre-mir26a-1,2-Forward:	TTCAAGTAATCCAGGATAGGCTGT	*

Pre-mir26a-1,2-Reverse:	TGCAAGTAACCAAGAATAGGCC	*
Pre-mir26b-Forward:	TTCAAGTAATCCAGGATAGGCTGT	*
Pre-mir26b-Reverse:	CAAGTAATGGAGAACAGGCTG	*
Pre-mir27a,b-Forward:	GCAGGGCTTAGCTGCTTG	*
Pre-mir27a,b-Reverse:	GGCGGAACTTAGCCACTGT	*
Pre-mir29a,c-Forward:	ATGACTGATTTCTTTTGGTG	*
Pre-mir29a,c-Reverse:	ATAACCGATTTCAGATGGTG	*
Pre-mir34a-Forward:	TGGCAGTGTCTTAGCTGGTTG	*
Pre-mir34a-Reverse:	GGCAGTATACTTGCTGATTGCTT	*
Pre-mir100-Forward:	AACCCGTAGATCCGAACTTG	*
Pre-mir100-Reverse:	TACCTATAGATACAAGCTTGTGCG	*
Pre-mir103-1,2-Forward:	GCTTCTTTACAGTGCTGCCT	*
Pre-mir103-1,2-Reverse:	TTCATAGCCCTGTACAATGCT	*
Pre-mir107-Forward:	CAGCTTCTTTACAGTGTTGCCT	*
Pre-mir107-Reverse:	GATAGCCCTGTACAATGCTGC	*
Pre-mir125b-1-Forward:	GTCCCTGAGACCCTAACTTG	*
Pre-mir125b-1-Reverse:	AGCCTAACCCGTGGATTT	*
Pre-mir125b-2-Forward:	GTCCCTGAGACCCTAACTTG	*
Pre-mir125b-2-Reverse:	AAGAGCCTGACTTGTGATGT	*
Pre-mir138-1,2-Forward:	CAGCTGGTGTTGTGAATCAG	*
Pre-mir138-1,2-Reverse:	ACCCTGGTGTCGTGAAATAG	*
Pre-mir145-Forward:	GTCCAGTTTTCCCAGGAATC	★
Pre-mir145-Reverse:	AGAACAGTATTTCCAGGAAT	★
Pre-mir191-Forward:	GCAACGGAATCCCAAAAG	*
Pre-mir191-Reverse:	GACGAAATCCAAGCGCA	*
Pre-mir192-Forward:	CTGACCTATGAATTGACAGCC	*
Pre-mir192-Reverse:	TGACCTATGGAATTGGCAG	*
Pre-miR193-Forward:	GTCTTTGCGGGCGAGAT	*
Pre-miR193-Reverse:	AACTGGGACTTTGTAGGCCA	*
Pri-mir21-Forward:	TTTTGTTTTGCTTGGGAGGA	
Pri-mir21-Reverse:	AGCAGACAGTCAGGCAGGAT	
Pri-mir31-Forward:	TGAGTGTGTTTTCCCTCCCT	*
Pri-mir31-Reverse:	GCCATGGCTGCTGTCAG	*
Pri-miR-192-Forward:	TGGTGGCGGGTAGTGGA	
Pri-miR-192-Reverse:	TGGCATTGAGGCGAACAT	
Pri-miR-193a-Forward:	ACCCCGAACTCCGAGGAT	
Pri-miR-193a-Reverse:	TGGGACTTTGTAGGCCAGTT	
EIF2C2-Q-Forward:	CACCATGTACTCGGGAGCC	
EIF2C2-Q-Reverse:	CAAAGTCGGGTCTAGGTGGA	
Dicer1-Q-Forward:	GAGCTGTCCTATCAGATCAGGG	
Dicer1-Q-Reverse:	ACTTGTTGAGCAACCTGGTTT	
ACTB-Q-Forward:	GCACAGAGCCTCGCCTT	Internal Control
ACTB-Q-Reverse:	GTTGTCGACGACGAGCG	Internal Control

Notes:

(1) For detection of mature miRNAs, TaqMan MicroRNA assay kits (Applied Biosystems) were used in accordance with the manufacturer's protocol.
(2) For pre-miR-31 detection, we used Hs_mir-31_1_PR miScript Precursor Assay (Qiagen) in accordance with the manufacturer's protocol.
(3) The primer sequences marked with "*" were from Jiang *et al*[49].
(4) The primer sequences marked with "★" were from Suzuki *et al*[26].

Oligonucleotide sequences for pMIR-Reporter

Oligonucleotide	**5′ to 3′**
miR-21-binding-F:	CTAGTTCAACATCAGTCTGATAAGCTAA
miR-21-binding-R:	AGCTTTAGCTTATCAGACTGATGTTGAA
miR-31-binding-F:	CTAGTAGCTATGCCAGCATCTTGCCTA
miR-31-binding-R:	AGCTTAGGCAAGATGCTGGCATAGCTA
miR-192-binding-F:	CTAGTGGCTGTCAATTCATAGGTCAGA
miR-192-binding-R:	AGCTTCTGACCTATGAATTGACAGCCA
miR-193a-5p-binding-F:	CTAGTTCATCTCGCCCGCAAAGACCCAA
miR-193a-5p-binding-R:	AGCTTTGGGTCTTTGCGGGCGAGATGAA
miR-31-192-193a-binding-F:	CTAGTCATCTTGCCTCATAGGTCAGCAAAGACCCAA
miR-31-192-193a-binding-R:	AGCTTTGGGTCTTTGCTGACCTATGAGGCAAGATGA

References

28 Huo, L. *et al.* RNA helicase A is a DNA-binding partner for EGFR-mediated transcriptional activation in the nucleus. *Proc Natl Acad Sci U S A* **107**, 16125-16130 (2011).

29 Parker, R. & Sheth, U. P bodies and the control of mRNA translation and degradation. *Mol Cell* **25**, 635-646 (2007).

30 Eulalio, A., Huntzinger, E. & Izaurralde, E. Getting to the root of miRNA-mediated gene silencing. *Cell* **132**, 9-14 (2008).

31 Gibbings, D. J., Ciaudo, C., Erhardt, M. & Voinnet, O. Multivesicular bodies associate with components of miRNA effector complexes and modulate miRNA activity. *Nat Cell Biol* **11**, 1143-1149 (2009).

32 Lee, Y. S. *et al.* Silencing by small RNAs is linked to endosomal trafficking. *Nat Cell Biol* **11**, 1150-1156 (2009).

33 Knodler, L. A. & Steele-Mortimer, O. The Salmonella effector PipB2 affects late endosome/lysosome distribution to mediate Sif extension. *Mol Biol Cell* **16**, 4108-4123 (2005).

34 Erler, J. T. *et al.* Lysyl oxidase is essential for hypoxia-induced metastasis. *Nature* **440**, 1222-1226 (2006).

35 Moreno-Manzano, V. *et al.* FM19G11, a new hypoxia-inducible factor (HIF) modulator, affects stem cell differentiation status. *J Biol Chem* **285**, 1333-1342 (2010).

36 Basu, R. K. *et al.* Interdependence of HIF-1alpha and TGF-beta/Smad3 signaling in normoxic and hypoxic renal epithelial cell collagen expression. *Am J Physiol Renal Physiol* **300**, F898-905 (2011).

37 Slomiany, M. G. & Rosenzweig, S. A. Hypoxia-inducible factor-1-dependent and -independent regulation of insulin-like growth factor-1-stimulated vascular endothelial growth factor secretion. *J Pharmacol Exp Ther* **318**, 666-675 (2006).

38 Ivan, M. *et al.* HIFalpha targeted for VHL-mediated destruction by proline hydroxylation: implications for O2 sensing. *Science* **292**, 464-468 (2001).

39 Rudel, S. *et al.* Phosphorylation of human Argonaute proteins affects small RNA binding. *Nucleic Acids Res* **39**, 2330-2343 (2011).

40 Levitzki, A. & Gazit, A. Tyrosine kinase inhibition: an approach to drug development. *Science* **267**, 1782-1788 (1995).

41 Anthis, N. J. *et al.* Beta integrin tyrosine phosphorylation is a conserved mechanism for regulating talin-induced integrin activation. *J Biol Chem* **284**, 36700-36710 (2009).

42 Hutchison, G. J. *et al.* Hypoxia-inducible factor 1alpha expression as an intrinsic marker of hypoxia: correlation with tumor oxygen, pimonidazole measurements, and outcome in locally advanced carcinoma of the cervix. *Clin Cancer Res* **10**, 8405-8412 (2004).

43 Debnath, J., Muthuswamy, S. K. & Brugge, J. S. Morphogenesis and oncogenesis of MCF-10A mammary epithelial acini grown in three-dimensional basement membrane cultures. *Methods* **30**, 256-268 (2003).

44 Hsu, S. C., Miller, S. A., Wang, Y. & Hung, M. C. Nuclear EGFR is required for cisplatin resistance and DNA repair. *Am J Transl Res* **1**, 249-258 (2009).

45 Lee, D. F. *et al.* IKKbeta suppression of TSC1 function links the mTOR pathway with insulin resistance. *Int J Mol Med* **22**, 633-638 (2008).

46 Varallyay, E., Burgyan, J. & Havelda, Z. MicroRNA detection by northern blotting using locked nucleic acid probes. *Nat Protoc* **3**, 190-196 (2008).

47 Hsu, J. M. *et al.* Crosstalk between Arg 1175 methylation and Tyr 1173 phosphorylation negatively modulates EGFR-mediated ERK activation. *Nat Cell Biol* **13**, 174-181 (2011).

48 Xia, W. *et al.* Nuclear expression of epidermal growth factor receptor is a novel prognostic value in patients with ovarian cancer. *Mol Carcinog* **48**, 610-617 (2009).

49 Jiang, J., Lee, E. J., Gusev, Y. & Schmittgen, T. D. Real-time expression profiling of microRNA precursors in human cancer cell lines. *Nucleic Acids Res* **33**, 5394-5403 (2005).